ROBERTA LERIN LOVISI

Steady-state solutions for multiphase flow elevation of oil, gas and water

São Paulo

2021

ROBERTA LERIN LOVISI

Steady-state solutions for multiphase flow elevation of oil, gas and water

Graduation work in Petroleum Engineering of the graduation course of the Mining and Petroleum Engineering Department from the Polytechnic School of University of São Paulo.

Concentration area: Petroleum production

Advisor: Prof. Dr. Rafael Gioria dos Santos

São Paulo

2021

Catalog Sheet

Lovisi, Roberta
Steady-state solutions for multiphase flow elevation of oil, gas and water / R. Lovisi -- São Paulo, 2021.
64 p.

Trabalho de Formatura - Escola Politécnica da Universidade de São Paulo. Departamento de Engenharia de Minas e de Petróleo.

1. Escoamento multifásico 2. Intermitência severa 3. Gradiente de pressão 4. Propriedades dos fluidos I. Universidade de São Paulo. Escola Politécnica. Departamento de Engenharia de Minas e de Petróleo II.t.

This work is dedicated to all of the children and adults that,

when little, dreamed of becoming scientists and inventors.

Acknowledgement

First of all I would like to thank my parents and sisters for the patience they had during all this year, during my graduation period and all my life. They were essential and helped me in the darkest and brightest of times.

I would like to thank my advisor, prof. Rafael Gioria, for having me as advisee. Apart from all difficulties, the path we had was essential for my personal growth and learning during the production of this work.

A special thanks to my friends that supported me during the graduation and made this phase of my life lighter and joyful.

I also want to thank my boyfriend for all of the times he supported and helped me continue when I thought there was no solution. He was like a lighthouse for me.

And last but not least, I want to thank all of the teachers and professors I had during my whole life. I could not have arrived here without them all, this achievement is not only mine, but theirs too.

Abstract

In the present work, it is presented an algorithm to integrate the hydrostatic pressure of multiphase fluids (oil, gas and water) along a pipeline in the ocean during a petroleum production process. The pressure analysis is essential to optimize the production and guarantee the correct dimension of the equipment, but the commercial models used to describe multiphase flows are usually very complex. Therefore the method proposed in this work comprehends a simpler but just as satisfying model to predict the pressure of the flow based on easy-to-measure characteristics.

This analysis is conducted in a linear and non-transient approach, in which the black oil model is used for the characterization of the liquid phase and the void fraction is defined by the drift flux described by Bhagwat and Ghajar (2013). The correlations for fluid properties from Standing (1947) and Ahmed (2001) and pressure drop approach from Chisholm (1973) are applied in the algorithm. The tests are done in a discretized riser and flowline of around 2000 meters depth with a lazy wave geometry, using field data from Andreolli (2018). The code presents an open source proposal and is written in Python.

As a result, the pressure integrated presents an error of around 20% in scenarios of low WOR, when compared to measured values, which is an acceptable value. Moreover, analyses of the GOR and flow rate show that lighter oils and higher rates present a higher pressure drop, and the algorithms can help predict those losses in order to dimensionate the flux. In general, the results contain several analyses of the gradient pressure related to some parameters of the flow and show a great repeatability and robustness of the algorithm.

Keywords: Multiphase flow, Severe slugging, Pressure gradient, Properties of fluids.

Resumo

No trabalho em questão, é apresentado um algoritmo que integra a pressão hidrostática em escoamentos multifásicos (óleo, gás e água) ao longo de dutos de produção de petróleo no oceano. A análise da pressão é imprescindível para otimizar a produção de petróleo e garantir o dimensionamento correto dos equipamentos, no entanto, os modelos usados para descrever escoamentos multifásicos em ambiente comercial costumam ser muito complexos. Por isso, o método proposto neste trabalho compreende um modelo mais simples, mas igualmente satisfatório, para prever a pressão do escoamento baseando-se em características fáceis de se mensurar.

A análise apresentada é conduzida com uma abordagem linear e não-transiente, na qual é usado o modelo de *black oil* para caracterização da fase líquida e a fração de vazio é definida pela proposta de *drift flux* de Bhagwat e Ghajar (2013). As correlações de propriedades dos fluidos de Standing (1947) e Ahmed (2001) além da abordagem de perda de carga de Chisholm (1973) são também implementadas no algoritmo. Os testes são realizados em um *riser* e *flowline* discretizados com cerca de 2000 metros de profundidade com uma geometria de *lazy wave* a partir dos dados de campo apresentados em Andreolli (2018). O código apresenta uma proposta aberta (*open source*) e é escrito em *Python*.

A integração da pressão apresenta erros da ordem de 20% para casos de baixo *WOR* quando comparados com os valores mensurados, o que é um erro aceitável. Além disso, análises das taxas de GOR e de vazão demonstram que óleos mais leves e com maiores fluxos têm uma perda de carga maior. Os resultados no geral contêm diversas análises do gradiente de pressão em relação a alguns parâmetros do fluxo e demonstram uma boa repetibilidade e robustez do algoritmo.

Palavras-chave: Escoamento multifásico, Intermitência severa, Gradiente de pressão, Propriedades dos fluidos.

Summary

List of Figures

List of Tables

List of Symbols

Alphabetic Symbols

a	Parameter of bubble pressure and solution gas-oil ratio equations [-]
A_1	Parameter of the water formation volume factor equation [-]
A_2	Parameter of the water formation volume factor equation [-]
A_3	Parameter of the water formation volume factor equation [-]
API	Oil specific gravity according to the American Petroleum Institute [°API]
B	Parameter of Chisholm correlation [-]
B_g	Gas formation volume factor [sm^3/sm^3]
B_o	Oil formation volume factor [sm^3/sm^3]
B_{ob}	Oil formation volume factor at bubble point [sm^3/sm^3]
B_w	Water formation volume factor [sm^3/sm^3]
C_0	Distribution parameter of the void fraction correlation [-]
$C_{0,1}$	Parameter of the void fraction [-]
C_1	Parameter of the void fraction [-] or First parameter of black oil model for conversion to S.I. [-]

C_2 Second parameter of black oil model for conversion to S.I. [-]

C_3 Third parameter of black oil model for conversion to S.I. [-]

D_h Inner diameter of the pipe [m]

f_{g0} Fanning friction factor of the gas phase [-]

f_{l0} Fanning friction factor of the liquid phase [-]

Fr_{sg} Froude number [-]

f_{tp} Fanning friction factor of the two-phase mixture [-]

g Gravity acceleration [m/s^2]

G Mass velocity [kg/m^2 s]

GOR Gas-oil ratio [sm^3/sm^3]

$GORI$ Injection gas-oil ratio [sm^3/sm^3]

j Total volumetric flux [m/s]

j_A Superficial velocity of the least dense of a two component mixture [m/s]

j_{AB} Drift flux of a two phase mixture [m/s]

j_B Superficial velocity of the most dense of a two component mixture [m/s]

j_m Superficial velocity of a two phase mixture [m/s]

La	Laplace variable [-]
n	Number of mols [-]
P	Pressure in the pipeline [Pa]
P_0	Pressure at standard conditions [Pa]
P_b	Bubble pressure [Pa]
P_{pr}	Pseudo reduced pressure [Pa]
P_{sep}	Pressure in the separator [bar]
P_{WCT}	Pressure in the wet christmas tree [bar]
R	Universal gas constant [J/kg K]
Re_{tp}	Reynolds number of the two phase mixture [-]
R_{so}	Solution gas-oil ratio [sm^3/sm^3]
T	Temperature [K]
T_0	Temperature at standard conditions [K]
T_{pr}	Pseudo reduced temperature [K]
V	Volume [m^3]
WOR	Water-oil ratio [sm^3/sm^3]

x	Horizontal distance [m]
z	Vertical distance [m] or Gas compressibility factor [-]
z_0	Gas compressibility factor at standard conditions [-]

Greek Symbols

α	Void fraction [-]
α_o	Superficial oil fraction [-]
α_w	Superficial water fraction [-]
β	Gas volumetric flow fraction [-]
ΔP	Pressure drop [Pa]
ΔP_A	Pressure drop due to acceleration loss [Pa]
ΔP_f	Pressure drop due to friction loss [Pa]
ΔP_H	Pressure drop due to static head [Pa]
Δz	Incremental axial elevation [Pa]
ϵ	Rugosity [m]
Γ	Physical property coefficient [-]

Y_o	Specific gravity of oil [-]
Y_{o0}	Specific gravity of oil at standard conditions [-]
$\bar{\mu}$	Average viscosity of the mixture [Pa/s]
μ_g	Viscosity of the gas phase [Pa/s]
μ_l	Viscosity of the liquid phase [Pa/s]
Φ_f^2	Two phase multiplier due to friction [-]
$\bar{\rho}$	Homogeneous density [kg/m^3]
ρ_g	Density of the gas [kg/m^3]
ρ_{g0}	Density of the gas at standard conditions [kg/m^3]
ρ_l	Density of the liquid [kg/m^3]
ρ_{l0}	Density of the liquid at standard conditions [kg/m^3]
ρ_o	Density of the oil [kg/m^3]
ρ_{o0}	Density of the oil at standard conditions [kg/m^3]
ρ_w	Density of the water [kg/m^3]
ρ_{w0}	Density of the water at standard conditions [kg/m^3]
σ	Surface tension of two fluids [N/m]

θ	Orientation of the pipe [rad]
x	Two phase flow quality [-]
X	Mass quality [-]

1. Introduction

Petroleum is an important commodity and one of the most used energy sources in the world. The oil, however, is a mixture of hydrocarbons, water and other molecules formed over a thousand years in very specific environments and conditions. Different authors classify it with different nomenclatures and compositions. The one that is going to be used in this work is the black oil, the most common type of petroleum produced, mainly on Brazil's coast. This kind of oil can have a variety of compositions, but normally it consists of large, heavy and nonvolatile molecules, and can have a color varying from brown to dark green (McCain, 2017).

It is usually found stored in rocks below the surface, either onshore and offshore, and it has always been a great challenge to find it and produce it. First of all because, as it does not rise spontaneously from the ground, one can not really affirm whether there is petroleum in some place without advanced geological and seismic techniques. Secondly, to access a reservoir and exploit the oil, it is necessary to drill the ground with heavy and sophisticated machinery.

In Brazil, the petroleum is exploited mostly on the coast under a water depth of up to 3000 meters. Due to the different conditions of the environments, the oil that comes from the reservoir passes through various transformations before reaching the platform on the surface. The initial one-phase mixture turns to a multiphase flow while flowing through the production pipelines. In this way through the flowline and riser, the petroleum can be identified as a mixture of oil, water and gas.

Usually the water and oil are considered the same liquid phase and the gas can be in solution in the liquid phase or free in a second phase, which is called void fraction. Depending on the pressure and temperature to which this mixture is subjected inside the lines, there can be more or less phases. When the black oil is inside the reservoir it is basically only oil, according to the model from McCain (2017), due to high pressure and temperature. When it is in a milder environment, with lower pressure and temperature, the gas that was in solution with oil is released and forms the void fraction, while the liquids tend to split in different phases because of the difference of density.

Due to the facts enunciated and the quantity of parameters, it is extremely complex to model a system of petroleum production. The multiphase flow presents also some additional challenges, such as instability due to downward flow, also known as severe slugging. This phenomenon is determined by the topography of the flowline and it is characterized by the cyclic formation of long slugs of liquid and quick expulsion of gas. It occurs on low flow rates, especially when a downward section (flowline) is followed by an upward section (riser), according to Andreolli (2018). The severe slugging can increase the pressure on the wellhead, trigger large instantaneous flows and flux oscillations in the reservoir.

All those effects can cause serious damage on the equipments and disturb the petroleum production if not treated correctly. So, in order to achieve the maximum oil production, it is important to predict when and where are the points with the most probability of suffering severe slugging and to implement the appropriate methods to avoid and/or correct the issue. One of the ways to identify it is to model the petroleum flow through the pipelines and map the curves of pressure, in function of some parameters.

1.1. Objective

This project has the purpose of mapping the hydrodynamic pressures of the petroleum flow inside production pipelines (flowline and riser). It will be achieved through implementing correlations for fluid properties and their mixtures using black-oil model, including processes of mass transfer, multiphase flow correlations for phase fraction and head losses. Finally, simulations of the oil production in order to map the pressures and to identify high and low pressure points and phase distributions will be done after validating the estimatives by comparing them with published data.

1.2. Justification

The pressure versus temperature diagrams are very important in the petroleum industry: they are used to optimize the production, to dimension the equipment and the system in general, and to assure the flow of hydrocarbons to the surface. The models used to describe the flow of fluids are usually mechanistic and very complex, which makes some simulations slow and inefficient. The method proposed in this work comprehends a simpler but just as satisfying model to predict the pressure of the flow based on some simple characteristics. Then, it is expected to contribute with the identification of points of greatest

adversities related to the oil pressure and to the understanding of the factors that lead to those highs and lows, so one can avoid them. Therefore it is expected to reduce the negative impacts of those phenomena and guarantee the maximum production of oil.

1.3. Structure of the present work

The introduction and contextualization of the work is presented in Section 1. In Section 2 there is a thorough review of the state of art of multiphase flows, in which some discussions are conducted about the instabilities of the flow, void fraction, pressure drop and correlations for properties of fluids. Still in Section 2 it is presented the numerical modeling of the problem and all of the equations used. Some of these equations are analysed graphically and compared with the literature results.

All those topics and correlations presented are used in the algorithm to integrate the pressure, which is shown in Section 3. There is the methodology of the work: the main steps of the integration, the field data and the discretized pipeline used to test it. The results and discussions are presented in Section 4 and, in Section 5, there are the conclusions and recommendations for future works.

2. Literature review

2.1. Multiphase flow

Multiphase flow is considered any flow with two or more phases or components. It can consist of different substances or the same one in different physical states, as steam-water and gas-oil. Multiphase flow can also be seen as gas-solid flows, in which gas drags little particles of dust, or also solid-liquid, in which liquids flow with bigger amounts of solids as ice or paraffin. It presents a more challenging modeling system than of a single-phase flow because of the different densities, compositions and flow patterns of the components, apart from other phenomena that only occur in this type of flow. In order to model it and predict the behaviour of the phases and its molecules, there are three main methods to do so, according to Brennen (2005):

i) experimentally, through physical prototypes;

ii) theoretically, using mathematical equations;

iii) computationally, using numerical models, great computational effort and power.

Most of the correlations and models known today are a result of experimental analyses and they rely basically on visual experiments and subjective judgement of their authors. Even so, they do not answer a great number of applications that would be unfeasible to try empirically, such as high pressure models and large scale phenomena. The computational and theoretical models are comparable to the experimental method as an alternative to working with scalable models and complex structures. However, they still have some downsides – it would be necessary to compute all of the details to the multiphase flow, to the particles' motions, arrange equations for each phase and for the interactions between components (Brennen, 2005). The computational processing to solve these problems is beyond the capacity used today and it would take too much time. Thus, creating reliable approximations is important to widen the applications without making the solutions so complex and unfeasible.

The geometry and topology of the environment can greatly influence some important aspects of the components, such as mass, momentum and energy transfer rates (Brennen, 2005). There is also a complex two-way coupling between the flow and its geometry, which is extremely difficult to model. Whereas the single-phase flow can have basically a laminar or turbulent regime, the multiphase flow can follow some patterns, which are specific

geometric distribution of components. Those patterns, or regimes, depend upon the inclination and rugosity of the pipe in which it flows and the mass quality *X* of the flux. The most common flow patterns in horizontal and vertical pipes are in bubbles, slug, plug, annular, stratified, disperse and wavy, which can be seen in Figure 1.

Figure 1 – Sketches of flow regimes for flow of air/water mixtures in a horizontal.

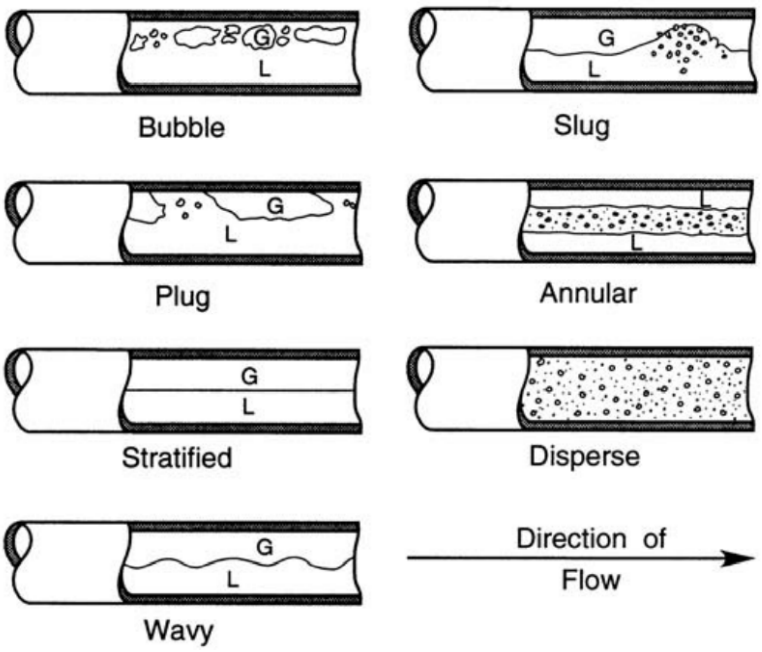

Source: Brennen (2005 apud Weisman, 1983).

The patterns are usually visually identified, but there are also other means of evaluation, such as spectral content of unsteady pressures or fluctuations in the volume fraction analysis, according to Brennen (2005 apud Jones and Zuber, 1974), that will not be discussed in this work. For simple flows, it is usually designed flow regime maps that relate the dependence of the flow pattern on component volume fluxes, on volume fraction and on fluid properties (density, viscosity and surface tension). The maps help to identify the likely pattern in a specific flow and they are plotted to given combinations of components and geometries. In Figure 2, it is possible to see the range of occurence of each regime in a flow of air-water as a function of their masses. There, the hatched zones are the transition regions between the regimes and the lines are the theoretical predictions. The patterns are subjected to small but significant aspects of the flow, such as the roughness, entrance and area of the pipe, Reynolds number etc., and even so, the transitions between them is not a delimited

condition, but a set of conditions. Because of that, the transitions are empirically defined as unstable regions with characteristics of both regimes around.

Figure 2 – Flow regime map for the horizontal flow of an air/water mixture.

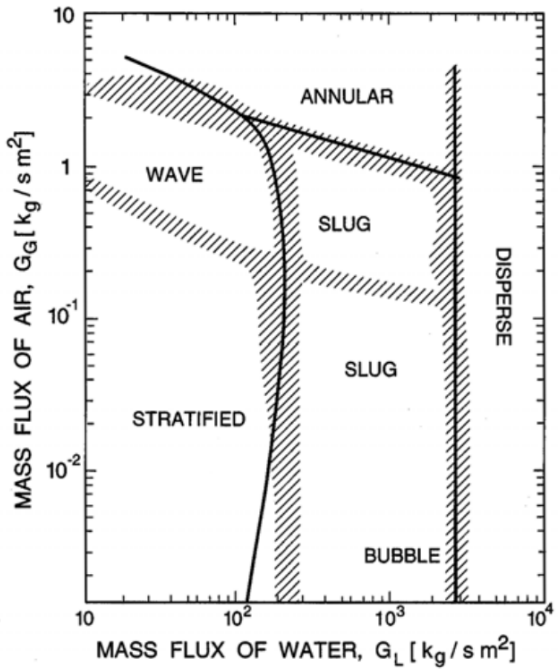

Source: Brennen (2005 apud Weisman, 1983).

2.1.1. Multiphase flow instabilities

Multiphase flows usually manifest instabilities that do not occur in single phase flows because of the nature of the composition of the mixture. According to Brennen (2005) the instabilities cause increase of pressure, flow rate or volume fraction oscillations in the flux that can disrupt the expected behaviour of the system and decrease the reliability and life of the machinery components. In the worst scenarios, it can also cause serious flow stoppage or structural failure.

One of the instabilities that can cause big damages in the petroleum industry is the severe slugging. It is characterized by a cyclical production of long liquid slugs and the quick release of great quantities of gas, as presented before, and is controlled mainly by gravity in the riser and compressibility in the flowline. The severe slugging occurs following some stages (Baliño et al., 2010), which are described below and can be seen in Figure 3.

Figure 3 – Stages of the severe slugging.

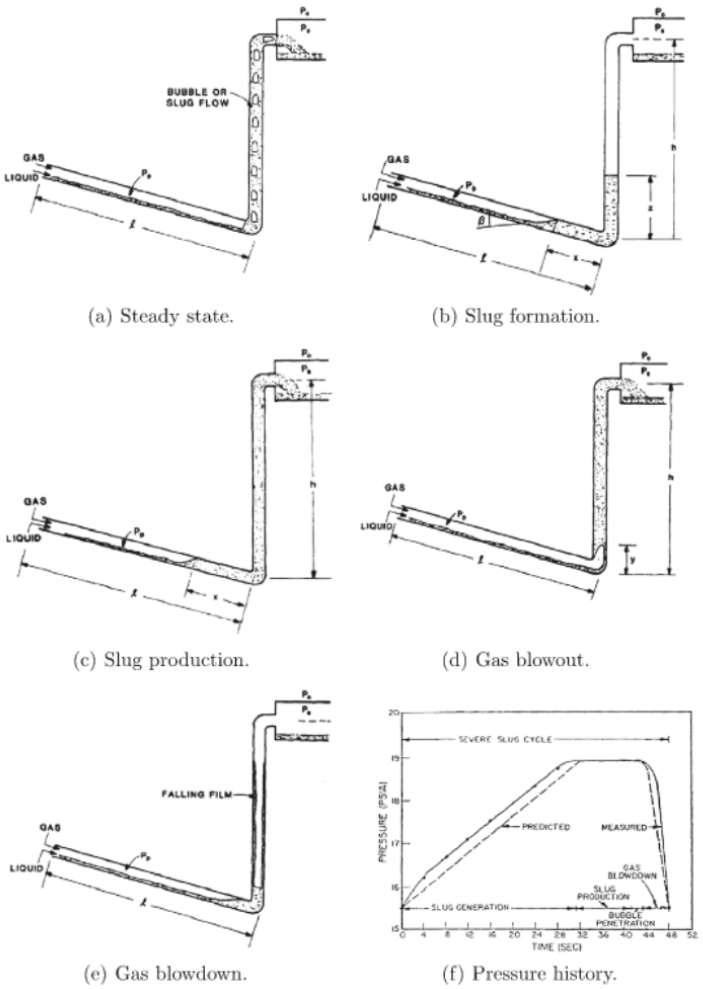

(a) Steady state. (b) Slug formation.

(c) Slug production. (d) Gas blowout.

(e) Gas blowdown. (f) Pressure history.

Source: Taitel (1986).

a) In the first stage, the flow is presented as bubbly and the state is steady.
b) As the system loses stability, the gas passage is blocked at the end of the flowline/bottom of the riser and the liquid continues to flow. All the gas in the riser flows out to the separator and the liquid is accumulated in the riser. The hydrostatic column becomes denser and the pressure at the bottom of the riser increases, which compresses the gas in the flowline.
c) When the liquid reaches the separator, there is no gas flowing there and the pressure reaches its maximum, that is the slug production stage.
d) As the liquid is flown to the separator, its accumulation front is pushed back until the bottom of the riser and the gas starts to flow through the riser, which is known as gas blowout.

e) As the gas flows through the riser, the pressure of the column decreases and there is a rapid decompression and violent expulsion of gas. This phenomenon is called gas blowdown.

2.1.2. Drift flux

Analysing a two-phase flow is not a simple task. It needs field equations for each of the components of the flux and equations that describe the dynamic relations and the relative motion between them. In the common two-fluid model, there are 6 field equations one has to arrange in order to model the flow's behaviour: a mixture and a gas continuity, two momentum equations and two energy equations. In addition to that, in practical applications, it is usually more common to have access to the information of the total mixture and not to each phase's data, but without all of the flow parameters it is not possible to calculate the equations of the proposed model. Furthermore, the modeling of the functions can become really complex and demand too much time, which is impractical in real-time simulations and analyses.

In order to work around this problem, the drift flux model is proposed by Zuber (1965) and Wallis (1969) as a simplification of the initial model: it allows to eliminate 2 equations from the system – an energy and a momentum equation. According to Goda et al. (2003), this model is one of the most accurate and practical for a two-phase flow and it has been extensively applied to related engineering problems. It is used to describe situations in which the relative motion of the components is governed by an external force – in most of the cases it is the gravity (Brennen, 2005). This model also considers that the mixture flows as a single-phase fluid and all of the parameters are obtained as a reflection of the whole, rather than two phases separately, according to Ishii and Hibiki (2006). Then, it is possible to see that the drift flux deals with the solution of the flow motion as a function of the external force g, of the volume fraction α and of the physical properties of the components, which is a reasonably good approximation.

As the drift flux is a simplification of the two-phase flow, some important characteristics of the flow are not taken into account in the equations. However, it still considers the relative velocity between the phases: they do not have to be coupled in this situation because the axial dimension of the systems is generally sufficiently large to enable interaction between components, as explained by Ishii and Hibiki (2006). The superficial

velocities of the phases are shown in Equation (1) and Equation (2) and are a function of the total volumetric flux j, the void fraction α and the drift flux j_{AB}.

$$j_A = \alpha . j + j_{AB} \tag{1}$$

$$j_B = (1 - \alpha) . j - j_{AB} \tag{2}$$

The convention defines that the component A is the least dense, so it represents the gas, and B is the most dense, so it will be the liquid. Expanding this concept, as α is the fraction of gas inside the pipe, it is related to the component A as it can be seen in Equation (3). The drift flux j_{AB} is then described in Equation (4), where u_{AB} is the relative velocity between the phases A and B, presented in Equation (5).

$$\alpha = \alpha_A = 1 - \alpha_B \tag{3}$$

$$j_{AB} = \alpha (1 - \alpha) u_{AB} \tag{4}$$

$$u_{AB} = u_A - u_B \tag{5}$$

The graphical representation of the relation among the variables in a drift flux model is presented in Figure 4. The right hand side of Equation (4) is equivalent to the straight dashed line which intercepts the known j_{AB} (α) curve. When connecting the j_A and $-j_B$ in each of the vertical axes (where $\alpha = 0$ and $\alpha = 1$) with the dashed line, the intersection with the j_{AB} (α), called operating point, defines the j_{AB} and α values (Brennen, 2005). The j_{AB} (α) function depends on the components of the flux.

Figure 4 – Graphical illustration of the drift flux model.

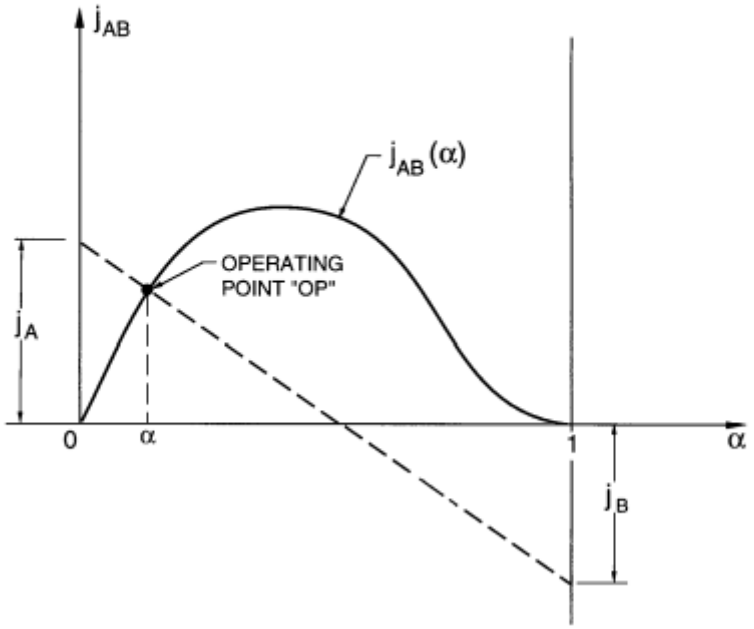

Source: Brennen (2005).

2.2. Void fraction

The void fraction (α), among all two-phase flow parameters (flow pattern, pressure drop, heat transfer, etc.), is one of the most important as it is used in almost all calculations of this type of flow. Nevertheless, the models that use void fraction are mostly developed to specific pattern flows (mainly horizontal and vertical orientations), or they need additional inputs related to the pattern flow. There are very little studies and correlations that can be applied to inclined pipes and to various combinations of components. Although it is possible to define the regime of the flow with graphical tools and mathematical equations, these are usually developed based on experimental observations. As mentioned above, visual observations are dependent on the individual experience and judgement of the researchers. Also, not in all of the times it will be possible to define beforehand the regime of the flow or it will not be really scalable, as there are conditions and combinations of components not yet studied.

Apart from that, preliminary research from Woldesemayat and Ghajar (2007) and Bhagwat and Ghajar (2012) showed that some recommended correlations of void fraction to some flow geometry tend to lose their accuracy in case of high pressure steam-water data,

very large diameter pipes and fluids with dynamic viscosity much higher than that of the water. In general, it lacks a closure relationship to predict the void fraction independent of the flow patterns, void fraction range, pipe diameter, pipe orientation and fluid properties (Bhagwat and Ghajar, 2013). Because of that, Bhagwat and Ghajar (2013) suggest a drift flux model correlation for calculating the void fraction that is independent of the flow pattern and pipe orientation over a wide range of system pressures, pipe, diameters and fluid properties. The one dimensional drift flux to determine void fraction is presented in Equation (6). There, α is the void fraction, j_A is the superficial velocity of the gas phase, C_0 is the distribution parameter, j_m is the mixture velocity and j_{AB} is the drift velocity. The < > and << >> symbols represent, respectively, the cross sectional averaged properties and the void weighted cross sectional area averaged flow properties.

$$\langle \alpha \rangle = \frac{\langle j_A \rangle}{C_0 \langle \langle j_m \rangle \rangle + \langle \langle j_{AB} \rangle \rangle} \tag{6}$$

In Equation (6), α is a function of the distribution parameter, presented as C_0 in Equation (7), and of the drift velocity, shown in Equation (12) as j_{AB}. One can see that C_0 is also dependent on α, which leads to a circular problem in order to find out the void fraction. Equation (7) contains as variables ρ_g and ρ_l, that are respectively the density of the gas and of the liquid, Re_{tp}, the Reynolds number of the two-phase flow, θ, which is the orientation of the pipe (0° is horizontal), and $C_{0,1}$, a parameter defined by Equation (8).

$$C_0 = \frac{2 - \left(\frac{\rho_g}{\rho_l}\right)^2}{1 + \left(\frac{Re_{tp}}{1000}\right)^2} + \frac{\left[\left(\sqrt{\left(1 + \left(\frac{\rho_g}{\rho_l}\right)^2 \cos\theta\right)/(1 + \cos\theta)}\right)^{1-\alpha}\right]^{\frac{2}{5}} + C_{0,1}}{1 + \left(\frac{1000}{Re_{tp}}\right)^2} \tag{7}$$

The $C_{0,1}$ parameter depends on the gas to liquid phase density ratio, the gas volumetric flow fraction (β), the two-phase flow quality (x), the two-phase friction factor (f_{tp}) and the constant C_1, which is equal to 0.2 when the pipe is circular and 0.4 when rectangular. Apart from that, calculating $C_{0,1}$ depends on the pipe orientation and the Froude number (Fr_{sg}). The Froude

number, according to Potter and Wiggert (2003), is a parameter that represents the gravitational effect of the flow. As it is seen in Equation (9), it is the ratio of inertial to gravitational force. It also contains the gravity value, g, and the diameter of the pipe, D_h.

$$C_{0,1} = \begin{cases} 0 & if\, 0^\circ \geq \theta \geq -50^\circ \, and \, Fr_{sg} \leq 0.1 \\ C_1 \left(1 - \sqrt{\frac{\rho_g}{\rho_l}}\right) \left[(2.6 - \beta)^{0.15} - \sqrt{f_{tp}}\right] (1 - x)^{1.5} & else \end{cases} \quad (8)$$

$$Fr_{sg} = \sqrt{\frac{\rho_g}{\rho_l - \rho_g}} \times \frac{J_{sg}}{\sqrt{g \,.\, D_h \,.\, \cos\theta}} \quad (9)$$

The two-phase friction factor (f_{tp}) is a value calculated by the Colebrook (1939) equation, shown in (10), and represents the pressure drop on the system due to friction. It is defined in terms of the relative rugosity of the pipe (ϵ/D_h) and the two-phase Reynolds number, that is used to identify whether the flow is laminar or turbulent. This formula also contains an iterative problem. The two-phase Reynolds number is presented on Equation (11) and, apart from the other variables already mentioned, is dependent on the dynamic viscosity of the liquid phase, μ_l.

$$\frac{1}{\sqrt{f_{tp}}} = -4 \log_{10} \left(\frac{\frac{\epsilon}{D_h}}{3.7} + \frac{1.256}{Re} \right) \quad (10)$$

$$Re_{tp} = \frac{j_m \, \rho_l \, D_h}{\mu_l} \quad (11)$$

The drift velocity is shown in Equation (12) and is a function of the pipe orientation, pipe diameter, fluid properties and void fraction. The components C_2, C_3 and C_4 represent an adjustment on the calculation, based on some conditions.

$$j_{AB} = (0.35\,sen\,\theta + 0.45\,\cos\theta)\sqrt{\frac{g\,D_h\,(\rho_l - \rho_g)}{\rho_l}} \times (1 - \alpha)^{0.5} \times C_2 \times C_3 \times C_4 \quad (12)$$

$$C_2 = \begin{cases} 2 & if\ \frac{\mu_l}{0.001} \leq 10 \\ \left(\frac{0.434}{\log_{10}(\mu_l/0.001)}\right)^{0.15} & else \end{cases} \quad (13)$$

$$C_3 = \begin{cases} 1 & if\ La \geq 0.025 \\ \left(\frac{La}{0.025}\right)^{0.9} & else \end{cases} \quad (14)$$

The Laplace variable (*La*) is shown in Equation (15) and Equation (16) adjusts the drift velocity to negative, if the pipe is tilted downwards, and to positive, in the opposite case. In the Laplace equation, σ is the surface tension of the fluids.

$$La = \frac{\sqrt{\sigma/[g\,(\rho_l - \rho_g)]}}{D_h} \quad (15)$$

$$C_4 = \begin{cases} -1 & if\ 0^\circ > \theta \geq -50^\circ\ and\ Fr_{sg} \leq 0.1 \\ 1 & else \end{cases} \quad (16)$$

2.3. Pressure Drop

In an ideal system, the energy is always conserved and the velocity and the flow flux would not be affected by friction, shear and other non-conservative elements. However, in every real application of multiphase flow there is pressure drop, either due to irregularities on the wall of the pipes, which are distributed and continuous, or because of some given components on the trajectory, which define punctual drops (Potter and Wiggert, 2003). Those effects are important because they have a great influence on the modeling of the system and with them it is possible to predict the behaviour of the flow and their components.

The pressure drop (ΔP), defined by the Equation (17), is a sum of friction loss (ΔP_f), static head (ΔP_H) and acceleration loss (ΔP_A). Those components are presented respectively

on Equation (18), Equation (19) and Equation (20). In Equation (18), f is the friction factor, that can be defined by the Colebrook equation (10), G is the mass velocity, D_h is the inner diameter of the pipe, Δz is the increment of axial elevation and ϕ_F^2, the two-phase multiplier. In Equation (19) and Equation (20), α is the void fraction of the flow, ρ_g is the density of the gas and ρ_l is the density of the liquid, g is the gravity, z is the vertical distance and x is the mass quality.

$$\Delta P = \Delta P_F + \Delta P_H + \Delta P_A \tag{17}$$

$$\Delta P_F = \frac{2fG^2}{\rho_l D_h} \Delta s \times \phi_F^2 \tag{18}$$

$$\Delta P_H = \{\alpha \rho_g + (1-\alpha)\rho_l\} \times g \times \Delta z \tag{19}$$

$$\Delta P_A = G^2 \left\{ \left(\frac{x^2}{\alpha \rho_g} + \frac{1-x^2}{(1-\alpha)\rho_l} \right)_{z+\Delta z} - \left(\frac{x^2}{\alpha \rho_g} + \frac{1-x^2}{(1-\alpha)\rho_l} \right)_z \right\} \tag{20}$$

In order to solve those equations, one can use the value of α, calculated by Equation (6), mass quality x, properties of fluids and of the system, that are already measured. However, the two-phase multiplier is an empirical correlation to adjust the pressure drop related to a continuous friction within the pipe. Different authors have dedicated themselves to define a correlation that best fits in the model proposed. Liu et al. (2013) evaluated various correlations and their performances in a steam generator under high pressures. The ones that best predicted the steam-water two-phase flow were the correlation from Friedel, which is already very common in literature, from Chisholm and the homogeneous model.

2.3.1. Correlation of Friedel

The Friedel two-phase multiplier is shown in Equation (21). There A_1, A_2 and A_3 are coefficients calculated by Equations (22), (23) and (24). This correlation is based on the Froude and Weber numbers, mass quality (x), density of the fluids (ρ_g and ρ_l), friction factors

for the total mass velocity G as all gas and all water (f_{g0} and f_{l0}), and the dynamic viscosity of the liquid and gaseous phase (μ_l and μ_g).

$$\phi_F^2 = A_1 + \frac{3.24 \times A_2 \times A_3}{Fr^{0.045} \times We^{0.035}} \tag{21}$$

$$A_1 = (1-x)^2 + x^2 \frac{\rho_l \times f_{g0}}{\rho_g \times f_{l0}} \tag{22}$$

$$A_2 = (1-x)^{0.224} \; x^{0.78} \tag{23}$$

$$A_3 = \left(\frac{\rho_l}{\rho_g}\right)^{0.91} \left(\frac{\mu_g}{\mu_l}\right)^{0.19} \left(1 - \frac{\mu_g}{\mu_l}\right)^{0.7} \tag{24}$$

In this correlation, both the Froude and the Weber numbers, presented respectively in Equations (25) and (26) use the homogeneous density $\bar{\rho}$, that is defined in Equation (27). The Weber number, similarly as how the Froude number relates inertial to gravitational forces, relates inertial forces to the forces of surface tension, which is represented as σ (Rapp, 2017).

$$Fr = \frac{G^2}{g \; D_h \; \bar{\rho}^2} \tag{25}$$

$$We = \frac{G^2 \, D_h}{\bar{\rho} \, \sigma} \tag{26}$$

$$\bar{\rho} = \frac{1}{\frac{x}{\rho_g} + \frac{1-x}{\rho_l}} \tag{27}$$

2.3.2. Correlation of Chisholm

Another correlation with good results is the one proposed by Chisholm (1973). The two-phase multiplier is presented in Equation (28). In this correlation, Γ is the physical property coefficient, defined by Equation (30), and *B* and *C* are parameters defined by Equation (31) and Equation (32).

$$\phi_F^2 = 1 + \left(\Gamma^2 - 1\right)\left\{B \times x^{\frac{2-n}{2}} \times (1-x)^{\frac{2-n}{2}} + x^{2-n}\right\} \tag{28}$$

$$n = \begin{cases} 0.25 & if\, Re \leq Re_{t1} \\ 0 & else \end{cases} \tag{29}$$

$$\Gamma = \left(\frac{\rho_l}{\rho_g}\right)^{0.5}\left(\frac{\mu_l}{\mu_g}\right)^{\frac{n}{2}} \tag{30}$$

$$B = \frac{C\Gamma - 2}{\Gamma^2 - 1} \tag{31}$$

$$C = 1 + \frac{x\,/\,\rho_g}{(x/\rho_g) + (1-x)/\rho_l} - \alpha \tag{32}$$

2.3.3. Homogeneous model

Differently from the other correlations, the homogeneous model considers the flow as single-phase and only considers the two-phase behaviour on properties such as viscosity and density (thermal properties), according to Liu et al. (2013). It happens because under high pressure conditions up to 18 MPa the steam-water flow behaves as a one-phase system, once their differences become very small. Thus the correlation does not include a two-phase multiplier in the calculus of the friction loss, but adjusts the viscosity and density as two-phase averaged properties: the average viscosity $\bar{\mu}$ is seen in Equation (33) and the density of the mixture ρ_m is shown in Equation (34).

$$\bar{\mu} = \frac{1}{\frac{x}{\mu_g} + \frac{1-x}{\mu_l}} \tag{33}$$

$$\rho_m = \rho_l (1 - \alpha) + \rho_g \alpha \tag{34}$$

Then, the Reynolds number, presented in Equation (35), is calculated with the two-phase average viscosity and it is used as input to the friction factor in the Colebrook equation. The new friction coefficient is then fed to Equation (18), the density used is the one defined by (34) and the two-phase multiplier is equal to 0. The new equation is shown in (36).

$$Re = \frac{G D_h}{\bar{\mu}} \tag{35}$$

$$\Delta P_F = \frac{2 f G^2}{\rho_m D_h} \Delta z \tag{36}$$

2.4. Properties of Fluids

The reservoirs are usually all different from each other: they consist of different types of rocks and fluids, and almost never will someone find two equal formations. Even so, some characteristics can be very similar to certain specific conditions, and because of that, and in order to standardize and facilitate the studies and analyses, there are classifications for the petroleum fluids. They are basically divided into reservoir models of gas and of oil. Among them there are other subtypes of fluids, which, according to McCain (2017), are: retrograde gas, wet gas, dry gas, volatile oil and black oil. It is very important to determine the fluid properly as there are properties and behaviours that influence greatly in the models and consequently in the results calculated. The one used in this work is the ordinary black oil. They are present in nearly every basin and constitute the majority of the petroleum produced around the world. Because it is heavy and there are large molecules in its composition, it is found as 100% liquid (or undersaturated) inside the reservoir, where the pressure and temperature are high.

In this case, it is assumed that the volume of fluids is a function only of the temperature and pressure. Thus if the pressure decreases under a specific constant temperature, the fluid, that was previously only liquid, releases gas until it reaches its minimum gas-oil ratio and there is only residual oil left. This characteristic is presented in the phase diagram of Figure 5.

According to El-Banbi et al. (2018) and McCain (2017), black oils present a gas-oil ratio (GOR) of less than 1750 scf/STB or have more than 20% of molecules with at least 7 carbon atoms (heavy molecules). Opposite to this, if the petroleum produces initially with a GOR higher than that and contains 20% or less of C7 molecules, it is considered a volatile oil. Yet, the distinction between them is very subtle. Because of that, El-Banbi et al. (2018) still divide the black oils into 2 categories: the low GOR and the moderate GOR oils, which have different characteristics and properties.

Nevertheless, the numerical attributes that define a black oil are not a consensus among authors in the literature. According to Ahmed (2001) the average gas-oil ratio for black oils is between 200-700 scf/STB, even lower than the one proposed by McCain (2017). Despite the quantitative differences, the models comply with some behaviours, and based on them one can determine the classification of the fluid. It is possible to see in Figure 5 that the bubble-point curve defines the transition zone in which the petroleum turns saturated, and the gas that was once solubilised in the oil is released as free vapor. This figure defines a typical black-oil phase diagram and is based on standard qualitative characteristics of the fluid.

A bubble-point is defined by a pressure at a given temperature below which the first bubble of gas is released, and over that the petroleum is completely liquid. There are different bubble-points for different temperatures, and all of them together define the transition curve from unsaturated to saturated fluid. Below this point the petroleum is characterized by the percent composition of liquid in the dashed lines, which are nearly equally distant from each other for the black oil model.

Figure 5 – Phase diagram of the ordinary black oil model.

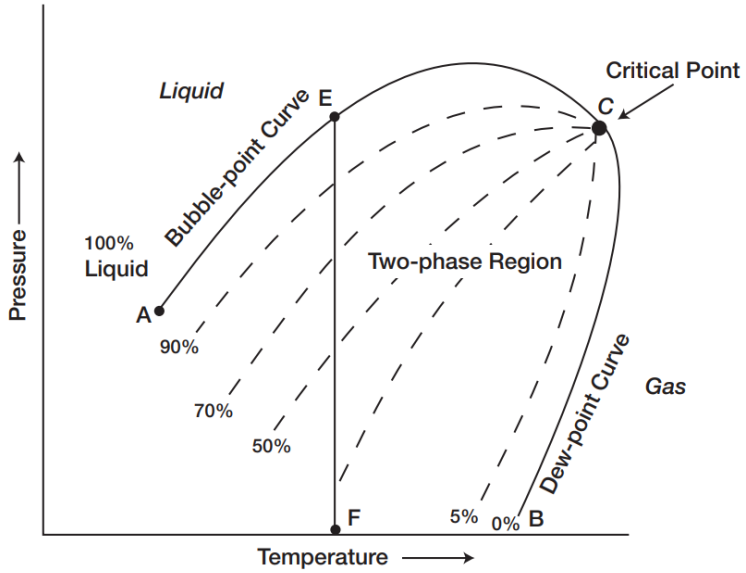

Source: Ahmed (2001).

Similarly to the bubble-point, however not so commonly discussed, the dew-point is defined as a pressure above which the first drops of oil are formed. And the critical point is the one at which gas and liquid coexist at an unstable balance. The point indicated by *E* in the figure represents the conditions found in a reservoir. In the black-oil model, they normally occur in the bubble-point or above it, and the temperature is usually much lower than in the critical point. During the production, the oil is subject to an isothermal transformation inside the reservoir, represented by the *EF* line, going from a high pressure condition to a low pressure one (point *F*), as the fluids are released from the rocks.

As the phase diagram presents a qualitative view of the properties, some authors have studied the correlations of the properties in order to calculate those values. Standing (1947) proposed some empirical correlations to the bubble pressure (P_b), solution gas-oil ratio (R_{so}) and the oil formation volume factor (B_o). Even though they are experimental, they have a good accuracy and applicability, and are still used until today. In those correlations, the coefficients C_1, C_2 and C_3 are used to adjust the units. The ones adopted here are related to the International System of Units (or SI) and have the following values: $C_1 = 5.61456349$ and $C_2 = 0.000145037738$, C_3 is defined in (39). Equation (37) presents the correlation for the bubble pressure and its coefficient a is shown in Equation (38).

$$P_b = \frac{18.2}{C_2}\left[\left(\frac{C_1\,R_{so}}{\gamma_g}\right)^{0.83} \times 10^{a} - 1.4\right] \tag{37}$$

$$a = 0.00091 \times C_3 - 0.0125 \times API \tag{38}$$

$$C_3 = 1.8 \times T - 459.67 \tag{39}$$

The API is one way of calculating the oil specific gravity, which represents the ratio of the oil density to the water density measured at the same environmental conditions, according to El-Banbi et al. (2018). The specific gravity γ is represented by the density of a substance (oil in this case) divided by the density of water, both at same conditions, and is dimensionless. The API gravity is commonly used in the petroleum industry to classify the quality of the oil and also for pricing it. The higher the API gravity, the lower is the density of the oil, and usually lighter fluids are more esteemed among consumers. Normally the API gravity for black-oils varies from 15° to 40° API. It can be calculated according to the Equation (40).

$$API = \frac{141.5}{\gamma_o} - 131.5 \tag{40}$$

The solution gas-oil ratio R_{so} is the quantity of gas produced to each barrel of oil. Once the reservoir is at or above the bubble pressure, the R_{so} remains constant and equal to the gas oil-ratio (*GOR*). In practice, however, most reservoirs, after a certain time, have their pressure decreased and thus the solution gas-oil ratio is also lower. A volatile oil, due to the presence of lighter molecules, usually presents a higher *GOR* than black oils. The *GOR* is the gas-oil ratio at standard conditions for a petroleum produced in a reservoir at bubble pressure. If it was produced at standard pressure and temperature conditions, defined as the surface, the *GOR* would be zero, as all of the gas would be already released (or non-existent). The typical curve for that property is shown in Figure 6 and defined in Equation (41).

$$R_{so} = \begin{cases} \frac{\gamma_g}{C_1}\left[\left(\frac{C_2\,P}{18.2} + 1.4\right) \times 10^{a}\right]^{1.2048} & if\ P < P_b \\ GOR & else \end{cases} \tag{41}$$

Figure 6 – Typical curve of the solution gas-oil ratio versus pressure.

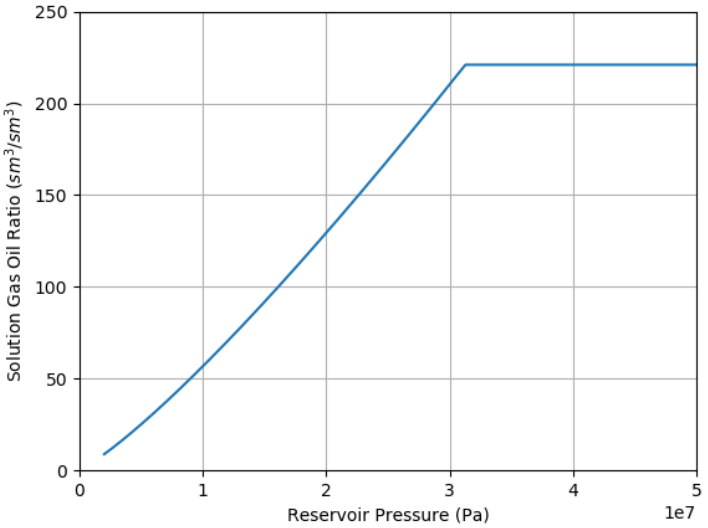

Source: author.

The oil formation volume factor is characterized by the volume of petroleum, considering oil and gas, at reservoir conditions required to produce one stock tank barrel of oil at the surface. Although two events occur when the petroleum reaches the surface – i) the release of free gas and ii) expansion of oil due to reduction of pressure and contraction due to reduction in temperature – only i) is relevant to the changes in volume of oil. In ii) the expansion and contraction of oil basically cancel each other and their effect is minimal (El-Banbi et al., 2018). This property is defined by Equation (42) and presented in Figure 7. Above the bubble-point, the oil formation volume factor decreases a little because of the expansion of oil due to the dissolved gas.

$$B_o = \begin{cases} 0.9759 + 0.00012\left[C_1\,R_{so}\left(\frac{\gamma_g}{\gamma_o}\right)^{0.5} + 1.25\,C_3\right] & if\ P < P_b \\ B_{ob}^{\,-\frac{-1433 + 5\,C_1\,GOR + 17.2\,C_3 - 1180\,\gamma g + 12.61\,API}{P \times 10^5}(P - P_b)} & else \end{cases} \tag{42}$$

Figure 7 – Typical curve of the oil formation volume factor versus pressure.

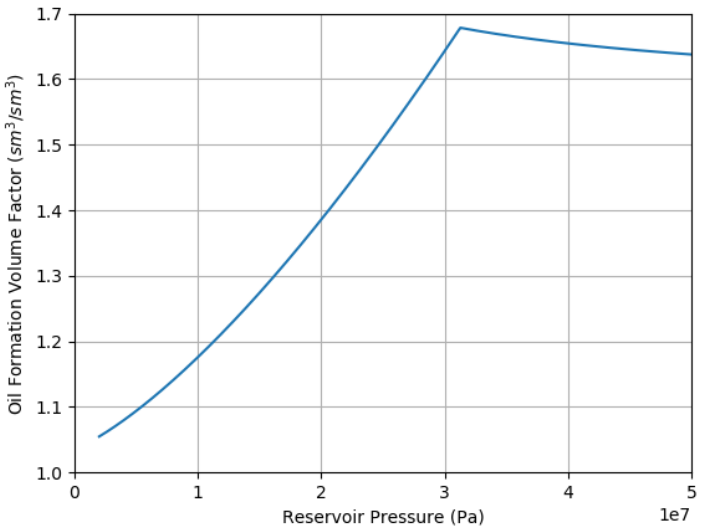

Source: author.

Another property used to characterize the fluids of petroleum is the water formation volume factor. In every hydrocarbon deposit there is water present, also known as brine, and it is produced along with oil and gas during the petroleum production process. The brine contains higher quantities of dissolved solids and ions than the seawater, according to Taha and Amani (2019), and the most common is the sodium chloride (NaCl). Due to the equilibrium between oil and water in the formation, the bubble pressure for both fluids is usually the same, however, the formation volume factors have very different behaviours.

The water formation volume factor is represented by B_w and is defined as the volume occupied by water and its dissolved gas in reservoir conditions for each stock tank barrel produced at standard conditions. According to Satter and Iqbal (2016), the water formation volume factor is usually very low, around 1.01 bbl/STB in typical cases. Similarly to the oil formation volume factor, B_w is subject to i) the liberation of free gas as the pressure is reduced, and ii) the expansion and contraction due to pressure reduction and temperature increase.

The solubility of gas in brine is much lower than in oil, so the gas is nearly all dissolved in the hydrocarbons rather than in water, which almost cancels the effect of i) in the depressurization of the formation water. The compressibility of water, relative to ii), on the

other hand, represents a greater effect than the release of gas, therefore the reservoir barrel of the formation water is relatively smaller than the surface barrel (Taha and Amani, 2019).

Ahmed (2001) presents an experimental expression that can be seen in Equation (43). Equation (44), Equation (45) and Equation (46) show the coefficients A_1, A_2 and A_3 from B_w and are defined for a gas-satured formation water. The pressure P is presented in Pascal and the temperature T in Fahrenheit. It is possible to see from Figure 8 that the water formation volume factor has a descendent behaviour as the pressure increases, just as discussed before.

$$B_w = A_1 + A_2 \times P + A_3 \times P^2 \tag{43}$$

$$A_1 = 0.9911 + 6.35 \times 10^{-5} \times T + 8.5 \times 10^{-7} \times T^2 \tag{44}$$

$$A_2 = -1.093 \times 10^{-6} - 3.497 \times 10^{-9} \times T + 4.57 \times 10^{-12} \times T^2 \tag{45}$$

$$A_3 = -5.0 \times 10^{-11} + 6.429 \times 10^{-13} \times T - 1.43 \times 10^{-15} \times T^2 \tag{46}$$

Figure 8 – Typical curve of the water formation volume factor versus pressure.

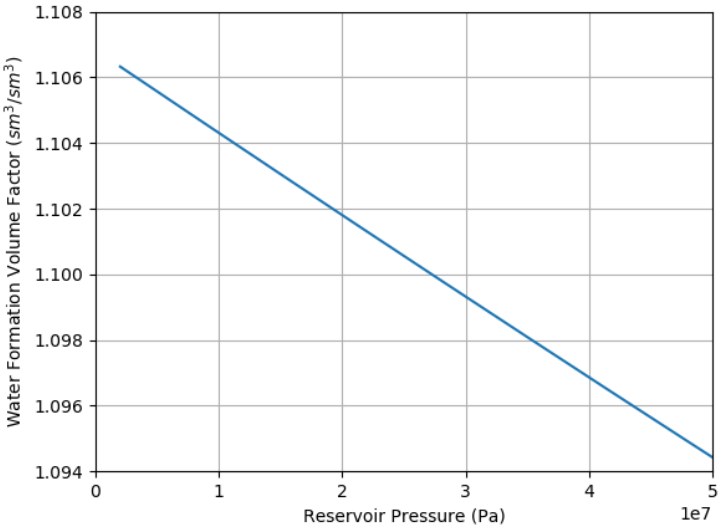

Source: author.

In addition to that, there is also the gas formation volume factor. That is another characteristic of the petroleum used to relate the volume of gas at a specified pressure and temperature to the volume of that same gas at standard conditions (in the petroleum industry it is considered as 60°F and 14.7 psia). Ahmed (2001) presents this relationship in Equation (47), there V is the volume in ft^3 at specific pressure and temperature conditions and V_0 is the volume at standard conditions in scf.

$$B_g = \frac{V}{V_0} \tag{47}$$

The equation above can be rewritten using the gas equation-of-state, presented in Equation (48). There P is the pressure of the gas in PSI, T is the temperature in Rankine, n is the number of moles, R is the universal gas constant and z is the compressibility factor, presented in Equation (50). When substituting Equation (48) into Equation (47), the new correlation can be seen in Equation (49) and its unit is sm^3/sm^3.

$$PV = nzRT \tag{48}$$

$$B_g = \frac{P_0\, T\, z}{P\, T_0\, z_0} \tag{49}$$

The correlation of z, according to Standing and Katz (1942), uses the pseudo reduced temperature and pressure of the oil to define the compressibility of gas, which, in turn, require the pseudo critical pressure and temperature. The correlations for pseudo critical properties were defined by Standing (1981) and are presented in Equation (51) and Equation (52).

$$z = 1 - \frac{3.52\, P_{pr}}{10^{\,0.9813\, T_{pr}}} + \frac{0.274\, P_{pr}^2}{10^{0.8157\, T_{pr}}} \tag{50}$$

$$P_{pr} = \frac{P}{P_{pc}} = \frac{P}{\frac{1}{C_2}\left(677 + 15\,\gamma_g - 37.5\,\gamma_g^2\right)} \tag{51}$$

$$T_{pr} = \frac{T}{T_{pc}} = \frac{T}{\frac{1}{C_5}\left(168 + 325\,\gamma_g - 12.5\,\gamma_g^2\right)} \tag{52}$$

It is possible to see in Figure 9, that the gas formation volume factor presents quite a small value compared to the water and oil volume factor. It happens because the compressibility of the gas is more sensitive to the pressure than the other elements. As the pressure gets higher, B_g tends to a value below 0.001 sm^3/sm^3, which means it is necessary to produce a large quantity of gas from the reservoir in order to have one barrel of gas in the platform. This behaviour is confirmed in Abdallah (2017)'s research, in which he presents data from various wells of petroleum production and their properties.

Figure 9 – Typical curve of the gas formation volume factor versus pressure.

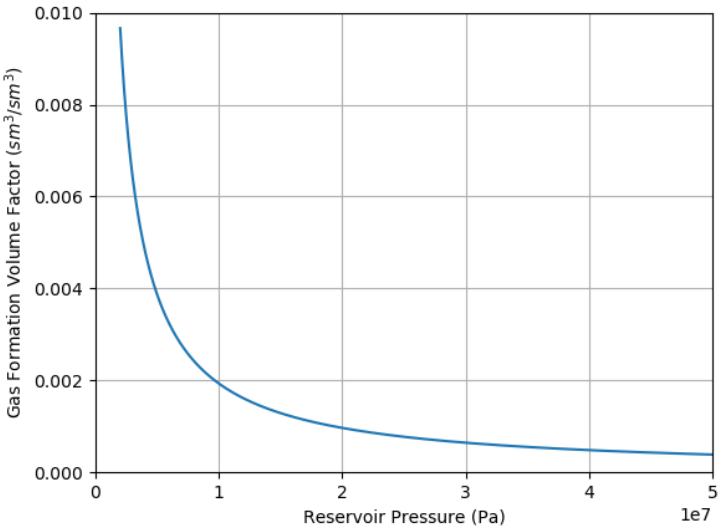

Source: author.

3. Methodology

The methodology proposed for the accomplishment of the work consists of calculating the pressure in discrete nodes of the pipes that take the petroleum from the wellhead until the platform by numerical integration of the pressure drop estimative (Section 2.3) which uses the estimative of void fraction introduced in Section 2.2. The evaluation of the pressures is done only at the platform and at the wet christmas tree, the pressures between those nodes are not analysed, as there is no measured value to compare to.

There are basically two kinds of pipes used for this purpose: the flowline, found laying on the seabed and almost horizontal, and the riser, that is suspended in the sea and has a predominantly upward orientation. In order to do so, the terms of the equation are analysed separately and each of them is calculated, graphically evaluated and compared to literature values for validation. Some articles and papers were reviewed (presented in Section 2) and their methods and equations selected so that proper correlations are applied to the model. In this way, it is expected that the final solutions present satisfactory results and refine preliminary calculations. This method aims to identify deviations and inappropriate applications beforehand.

In order to compare the results, it is compared the differences in forward and backward integrations of the pressure, which means respectively the integration from the platform to the wet christmas tree and the opposite direction. As noted by Andreolli (2018), the discretization of the pipeline in more or less nodes does not have a big influence on the result of the integration. When increasing from 10 to 100 nodes, the standard error decreased from 1,5% to 0,5%, which is not significant. Then, in this work it was only analysed how the two-phase multiplier (from Chisholm and from Friedel) and the physical and chemical characteristics influence the results, but not the discretization of the pipe.

3.1. Correlation tests and assumptions

In order to solve the problem of the pressure along the production pipelines, primarily all of the correlations and properties used in the expression were modeled and calculated separately using the literature data analysed. The correlations used are the ones discussed in prior sections: void fraction and drift flux from Bhagwat and Ghajar (2013), properties of

fluids from Standing (1947) and Ahmed (2001) and for pressure drop it was considered the approaches from Friedel (1979) and from Chisholm (1973). Their results and graphical representation were calculated and computed using the data from Andreolli (2018) and Liu et al. (2013), and then compared with the results obtained in the books and papers consulted.

3.2. Integral of the solution

The hydrostatic pressure of the fluid inside the production pipe increases as it approaches the lower point at the seabed level. However, this increase in pressure is not linear and it depends on the vertical distance of the point considered to the surface and on the properties of the petroleum, such as the density. The gradient pressure defines the incremental amount of pressure to an infinitesimal distance. It is calculated according to the Equation (53) and integrated for small distances at various iterations.

$$\frac{\partial P}{\partial S} = -\rho_m \cdot g \cdot \sin\theta - \phi_f^2 \cdot \frac{f_l}{2} \cdot \frac{G^2}{\rho_L \cdot D_h} \tag{53}$$

The properties of the fluid, on the other hand, also depend on the pressure, so at each iteration, the parameters of the multiphase flow are calculated according to the new pressure and used again to integrate the gradient. This process is executed until it reaches the christmas tree at the bottom, or the surface in the opposite direction: starting from the christmas tree and reaching the separator. An illustrative example of the riser and flowline at which the pressure is integrated is presented in Figure 10.

Figure 10 – Geometry of petroleum production pipes.

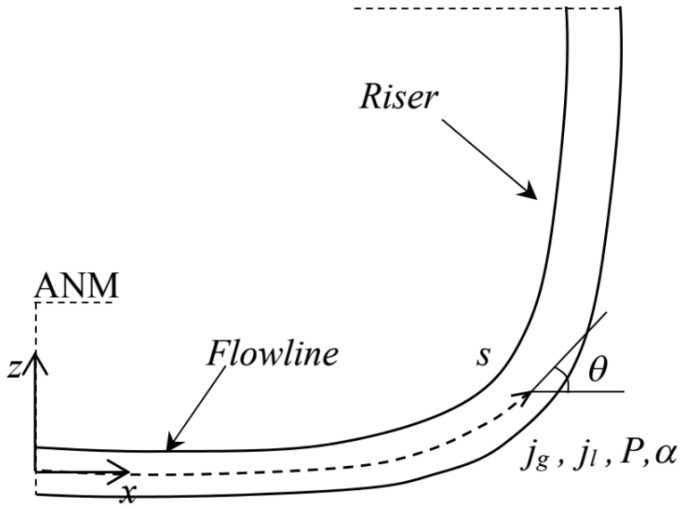

Source: Adapted from Andreolli (2018).

In Equation (53), ρ_m is the density of the mixture, which comprehends oil, gas and water, and its correlation is presented in (54), ρ_l is the density of the liquid phase, presented in (55) and g is the gravity acceleration (considered 9.81 m/s^2). The void fraction α and the two-phase multiplier Φ are calculated using the correlations presented in Sections 2.2 and 2.3, whereas a relation among the gas (α), oil (α_o) and water (α_w) fractions is defined in (56). Some other data are measured in the field and are presented in the next section, Equations (57) and (58) show how to calculate the oil and water fraction in the pipes.

$$\rho_m = \rho_g \alpha + \rho_o \alpha_o + \rho_w \alpha_w \tag{54}$$

$$\rho_l = \frac{\rho_o \alpha_o + \rho_w \alpha_w}{1 - \alpha} \tag{55}$$

$$\alpha + \alpha_o + \alpha_w = 1 \tag{56}$$

$$\alpha_o = \frac{j_o}{j_o + j_w} (1 - \alpha) \tag{57}$$

$$\alpha_w = \frac{j_w}{j_o + j_w}(1 - \alpha) \tag{58}$$

The densities of water and oil at flow condition are calculated according to Equation (59) and Equation (60) respectively. There ρ_{w0}, ρ_{o0} and ρ_{g0} are the densities of water, oil and gas at standard conditions respectively; ρ_{w0} is equal to 999.14 kg/m^3, ρ_{o0} and ρ_{g0} are shown in Equation (61) and Equation (62). In Equation (61), γ_{o0} is the specific gravity of oil at standard conditions, in Equation (62) z is the compressibility factor of real gases, defined in Equation (50), and the specific gas constant for dry air R is equal to 287.058 J/kg.K. Those data are from Andreolli (2018).

$$\rho_w = \frac{\rho_{w0}}{B_w} \tag{59}$$

$$\rho_o = \frac{\rho_{o0} + \rho_{g0}\, Rs_o}{B_o} \tag{60}$$

$$\rho_{o0} = \gamma_{o0}\, \rho_{w0} \tag{61}$$

$$\rho_{g0} = \frac{P}{R\, T\, z} \tag{62}$$

Some other important parameters to the solution of the expressions are the superficial velocities of the fluids (j_w, j_o and j_g), which are presented in Equation (63), Equation (64) and Equation (65). They are measured in m/s and through them it is possible to define the drift flux of the mixture. There B_w, B_o and B_g are the water, oil and gas formation volume factors, shown in Equation (43), Equation (42) and Equation (47), *WOR* is the water-oil ratio, *GOR* is the gas-oil ratio, j_{o0} is the superficial velocity of oil at standard conditions and R_{so} is the solution gas-oil ratio (Equation (41)).

$$j_w = B_w \times WOR \times j_{o0} \tag{63}$$

$$j_o = B_o \times j_{o0} \tag{64}$$

$$j_g = B_g \times j_{o0} \times (GOR - R_{so}) \tag{65}$$

In order to integrate Equation (53), the parameters are calculated at each iteration of the system, all along the length of the pipe (considering the riser and the flowline). The correlation for void fraction is based on the one proposed by Bhagwat and Ghajar (2013) and the two-phase multiplier is based on Chisholm's, presented by Liu et al. (2013). The characteristics of the fluids and the flow are calculated as above. The heights in each iteration are equally distributed and presented in Section 4.0.

3.3. Field data

The input data used to integrate the pressure along the pipes were obtained from Andreolli (2018) and presented in the tables below. Table 2 presents the data measured in different scenarios, each one considered a single simulation, at the separator (variables with sub-index *sep*) or at the wet christmas tree (variables with sub-index *WCT*) used as boundary conditions.

All of the simulations are applied to the pipeline whose discretized points are presented in Table 1, and its profile is shown in Figure 11. The column with the θ values in Table 1 are calculated according to the geometry of Figure 10 and the expression is presented in Equation (66), there z_i is the height of the i-th point and x_i is the horizontal distance from this point to the wet christmas tree.

$$\arctan \frac{z_i - z_{i-1}}{x_i - x_{i-1}} \tag{66}$$

Table 1 – Discretized points of the riser's profile.

Localization	Distance (m)	Height (m)	Theta (°)
Platform	7563	2159	90,00

Riser	7563	2129	90,00
Riser	7513	1779	81,87
Riser	7463	1579	75,96
Riser	7363	1279	71,57
Riser	7263	1079	63,43
Riser	7163	979	45,00
Riser	7063	929	26,57
Riser	6963	949	-11,31
Riser	6863	979	-16,70
Riser	6763	904	36,87
Riser	6713	804	63,43
Riser	6663	559	78,47
Riser	6613	379	74,48
Riser	6563	279	63,43
Riser	6463	99	60,95
Riser	6363	9	41,99
Riser	6313	-11	21,80
Flowline	6263	-11	0,00
Flowline	5885	-11	0,00
Flowline	1	0	-0,11
WCT	0	0	0,00

Figure 11 – Pipe's profile (riser and flowline).

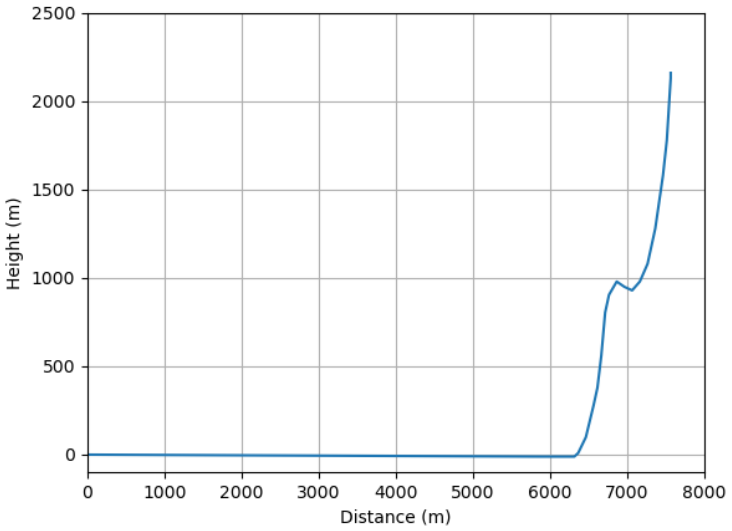

Source: author, using data from Andreolli (2018).

Table 2 – Input data for the integration of the pressure gradient.

# Simulation	j_{o0} (m/s)	P_{WCT} (bar)	P_{sep} (bar)	GOR (sm^3/sm^3)	WOR	T (K)
1	1,88	201,00	41,60	221,10	0,00	308,70
2	1,67	203,60	52,20	223,90	0,00	308,80
3	1,86	175,00	25,00	212,40	0,01	307,70
4	1,42	145,00	23,20	223,70	0,05	308,70
5	1,23	131,90	22,60	221,90	0,10	306,60
6	1,17	128,10	22,30	218,10	0,11	306,60
7	1,13	125,80	22,20	214,80	0,14	306,60
8	1,10	122,40	22,00	214,30	0,14	306,40
9	0,89	114,70	21,60	220,20	0,19	306,00
10	0,81	111,50	21,40	228,80	0,19	305,90
11	0,79	109,80	21,40	223,70	0,21	305,70

4. Results

4.1. Pressure integration

In this Section, it is presented the result of the pressure integration for each of the scenarios presented in Table 2. The integration was executed using a library in Python that solved the Equation (53) for the discretized points in Table 1. Here, the algorithm started the calculations from the separator, using its boundary conditions, until reaching the wet christmas tree. Figure 12 presents the pressure profile of the fluids inside the pipelines versus its length from the platform to the christmas tree (wet christmas tree is at 0 m). It is possible to see that the curve of the graph behaves as expected: in the separator the pressure is very low and, as it is closer to the seabed, the pressure increases. Around the point 6700 m, it is possible to see that there is an oscillation of the pressure due to the lazy wave of the riser. Lazy wave is a geometry used in ultradeep oil production, as presented in Figure 11, that can reduce the mechanical tension in the riser and avoid damage to the equipments on the platform. Finally, in the flowline the pressure is almost constant, as the height is basically the same. In the data from Simulation 1 of Table 2, and applying the Chisholm two-phase multiplier correlation, using the initial pressure of 4.16 MPa the final value achieved was 24.22 MPa against 20.10 MPa of the measured data. The difference, using Equation (67), is about -20.47%, which means the algorithm achieved a pressure almost 20% higher than the measured one.

$$error = \frac{P_{measured} - P_{estimated}}{P_{measured}} \tag{67}$$

The pressure profile was not computed for all of the simulations as the general shape of the curve is almost the same, once the same pipeline is used in all of them. However, the error of the estimated pressure differs a lot in each simulation, and it is discussed in Section 4.4.

Figure 12 – Result of the forward integration of the pressure versus the length of the pipe in Simulation 1 of Table 2 using Chisholm correlation.

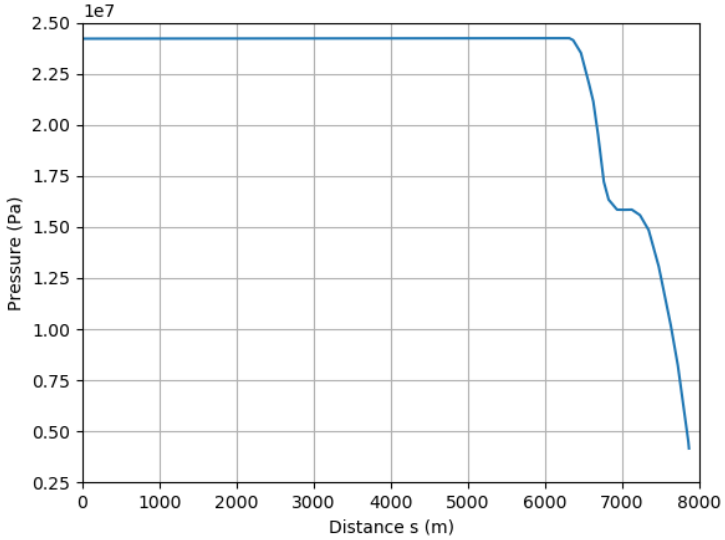

Source: author.

4.2. Comparison of forward and backward integration

In order to test the algorithm, the same integration was executed backwards: starting from the wet christmas tree until reaching the platform, the result can be seen in the comparison of the integrations in Figure 13. The integration of the system should be independent of the direction of calculus and the result for both directions should be almost the same – this is what happens in the graph of Figure 13. The general format from the curves is preserved and they are shifted around 5 MPa from one another. This means that the integration method is robust and the equation is correctly employed. Then, it is possible to use this algorithm to calculate both the pressure at the platform and at the wet christmas tree, depending on the data available.

Figure 13 – Comparison of the results of the forward and backward integration of the pressure versus the length of the pipe in Simulation 1 from Table 2 using Chisholm correlation.

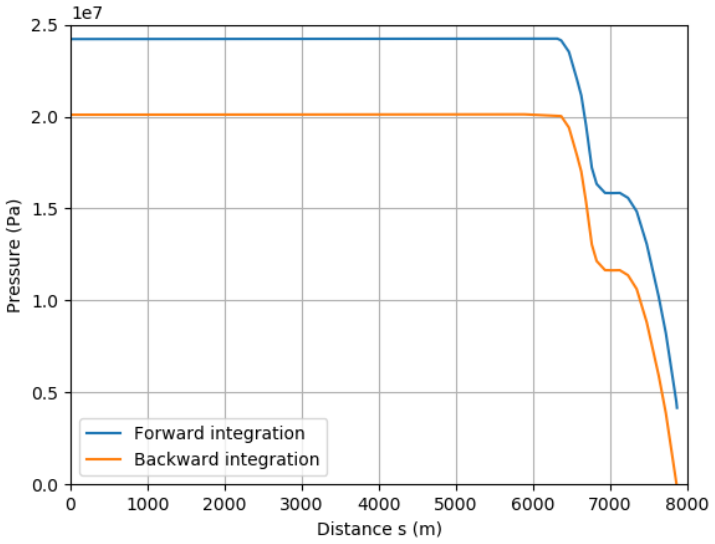

Source: author.

4.3. Comparison of two-phase multipliers

As presented in Section 2.3, Liu et al. (2013) compares some two-phase multipliers. In this work, it was used mainly the Chisholm correlation, as it is an alternative to the already known Friedel correlation. However, the results of both of them are compared with the purpose of evaluating which one presents indeed the best results. In Table 3 it is possible to see in the last 2 columns the error of both two-phase multiplier correlations for each simulation and in Figure 14 they are compared using the data from Simulation 1.

Table 3 – Error of the estimated pressure of correlations of Chisholm and Friedel for each simulation from Table 2.

# Simulation	P_{WCT} (bar)	P_{sep} (bar)	GOR (sm^3/sm^3)	Chisholm error	Friedel error
1	201,00	41,60	221,10	-20.47%	-26.48%
2	203,60	52,20	223,90	-19.11%	-23.25%
3	175,00	25,00	212,40	-30.58%	-40.30%
4	145,00	23,20	223,70	-45.95%	-55.07%
5	131,90	22,60	221,90	-56.05%	-64.33%
6	128,10	22,30	218,10	-58.93%	-66.78%
7	125,80	22,20	214,80	-61.35%	-69.01%
8	122,40	22,00	214,30	-64.71%	-72.22%
9	114,70	21,60	220,20	-70.90%	-77.08%
10	111,50	21,40	228,80	-73.89%	-79.68%
11	109,80	21,40	223,70	-76.15%	-81.66%

Figure 14 – Comparison of the results of the Chisholm and Friedel correlations in Simulation 1 from Table 2.

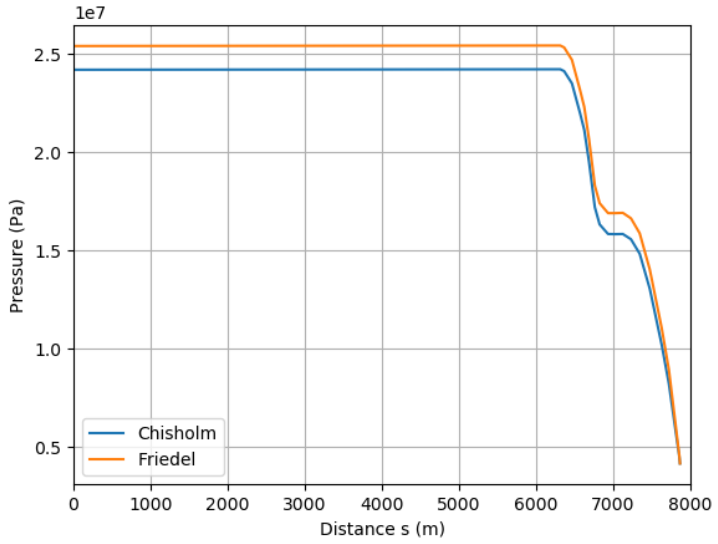

Source: author.

One can infer that the difference between them is not so significant, but yet the Friedel two-phase multiplier presents a higher error in most of the cases, even though it is the most known and used correlation in the petroleum industry. Because of that, the Chisholm pressure drop correlation is used in this work as the standard correlation coefficient.

4.4. Analysis of error

Whereas it was not plotted all of the simulations, the errors of the estimated pressure in the direct integration were computed and presented below with the purpose of analysing and understanding how it is behaving throughout the simulations. Table 4 presents the error of the estimated pressure in relation to the measured pressure at the wet christmas tree using Chisholm two-phase multiplier.

Table 4 – Error of the estimated pressure for each simulation from Table 2.

# Simulation	P_{WCT} (bar)	P_{sep} (bar)	GOR (sm^3/sm^3)	Error of the estimated pressure
1	201,00	41,60	221,10	-20,47%
2	203,60	52,20	223,90	-19,11%
3	175,00	25,00	212,40	-30,58%
4	145,00	23,20	223,70	-45,95%
5	131,90	22,60	221,90	-56,05%
6	128,10	22,30	218,10	-58,93%
7	125,80	22,20	214,80	-61,35%
8	122,40	22,00	214,30	-64,71%
9	114,70	21,60	220,20	-70,90%
10	111,50	21,40	228,80	-73,89%
11	109,80	21,40	223,70	-76,15%

In order to understand the reason for this difference, it was calculated the correlation between some of the parameters in Table 2 and the errors. The correlation is calculated according to Equation (68) and the result of this analysis is presented in Table 5. In Figure 15

it is possible to see the normalized value of the parameters (vertical left axis) in each simulation (horizontal axis) confronted with the errors (vertical right axis).

$$correl\,(X,\,Y)\;=\;\frac{\Sigma(x\,-\,\bar{x})(y\,-\,\bar{y})}{\sqrt{\Sigma(x\,-\,\bar{x})^{2}\,\Sigma(y\,-\,\bar{y})^{2}}} \tag{68}$$

Table 5 – Correlation from some parameters with the error.

Parameter	j_{o0}	GOR	WOR	T
Correlation with error	96,87%	-13,16%	-97,24%	92,48%

Figure 15 – Values of some parameters and of the error for each simulation from Table 2.

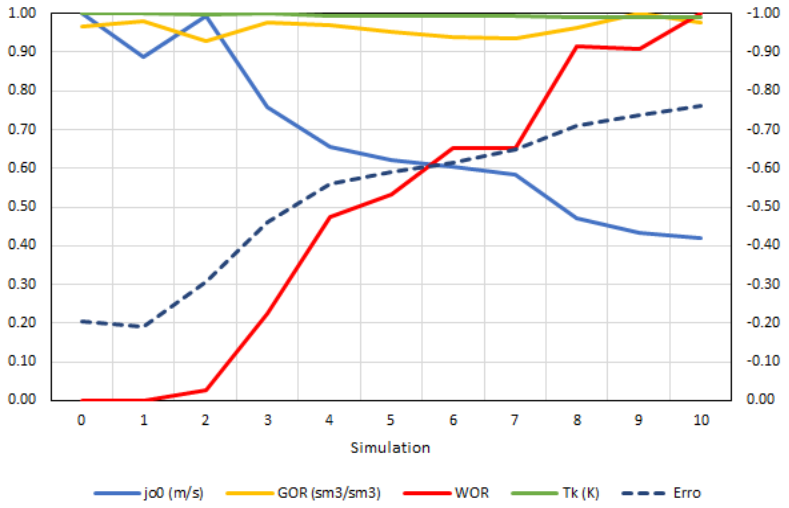

Source: author.

It is possible to infer that the main cause of errors is the *WOR*. It is seen in both the graph from Figure 15 and in Table 5, in which the absolute correlation between error and *WOR* is the highest among the parameters. As the water-oil ratio increases, the error increases in the negative axis (the estimated pressure is higher than the measured value). This assumption is reasonable once the model for water properties is not very robust and does not include variations of density and viscosity, for example. Along the riser, the change in

pressure and temperature can also change the properties of water, but in this work those properties are considered constant.

The temperature (T) and superficial velocity of oil at standard conditions (j_{o0}) also have a large correlation with the error. However, the temperature varies little in each simulation and the difference among them is not large enough to observe those errors, and j_{o0} can be the cause of the error, but may also have a coincident behaviour with the error. Thus, in this case, it is considered as the main cause of errors the increase in the water-oil ratio.

4.5. Analysis of GOR quantity in the oil

In addition to the previous results, the pressure was plotted to different values of gas-oil ratio with the purpose of analysing the influence of *GOR* in the final result of the problem. The integration started in the platform with the same values of Simulation 1 from Table 2 and continued until reaching the wet christmas tree; all other variables (except for *GOR*) were kept constant. The result is presented in Figure 16. To higher values, as the *GOR* increases, the distance between the curves also increases. As there is more gas dissolved in the oil, the mixture becomes lighter but more volatile, which also increases the general pressure inside the pipeline. Heavier fluids are less subject to height and temperature along the ocean's depth, which represents less tension in the pipe's inside walls.

Figure 16 – Charts of the integration of the pressure versus the length of the pipe in Simulation 1 to different GOR values.

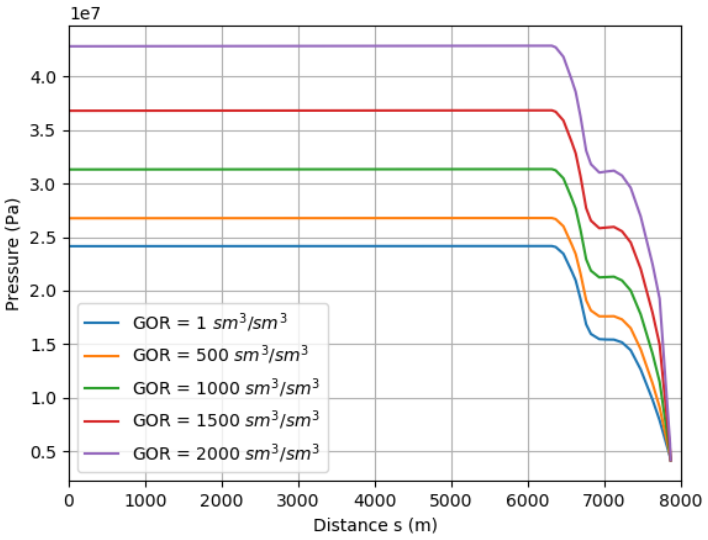

Source: author.

4.6. Analysis of the flow rate

An important way to evaluate the performance of the oil production is plotting the pressure against the flow rate of the fluids. The engineers and managers of a petroleum field use the flow rate to analyse how the production is going and plan the whole process and activities. The higher the flow rate, the higher is the amount of petroleum produced. However, the pressure inside the pipelines gets also higher as the flow rate increases and can cause problems during the production, as discussed above. Then, Figure 17 shows the curves for Simulation 1 of the pressure as a function of the distance from the wet christmas tree. The flow rate, which uses Chisholm's correlation, is calculated according to Equation (69). One can see that, as the flow rate increases, the pressure also increases, once there are more fluids flowing inside the same area.

$$Q_0 = j_{o0} \times A = j_{o0} \times \pi \times \left(\frac{D_h}{2}\right)^2 \tag{69}$$

Figure 17 – Pressure plotted against distance from wet christmas tree to various values of flow rate using data from Simulation 1 and Chisholm two-phase multiplier.

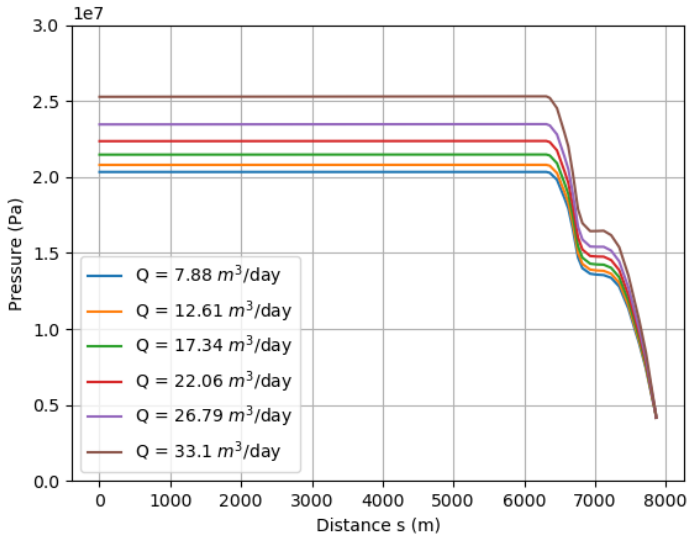

Source: author.

Another important data that is considered in the analysis of the oil production are the Tubing Performance Relationship curves (TPR curves). They are used in nodal analyses and show the expected behaviour of the fluids in a specific node to various values of flow rate. In this case, it is analysed the wet christmas tree's pressure profile, which is presented in Figure 18, using data from Simulation 1 and both two-phase multiplier correlations: from Chisholm and from Friedel.

It is possible to see that, as the flow rate decreases, the pressure also reaches a lower value, while it increases in a parabolic manner when the flow rate increases. The increase of the pressure is not so significant in the lower values of the flow rate because the friction with the tube is very high to lower fluxes and the pressure loss is equally high. However, as the inertia is overcome, the friction is not so relevant, thus the pressure has an ascendent behaviour.

Figure 18 – TPR curves for Simulation 1 using Chisholm and Friedel two-phase multiplier.

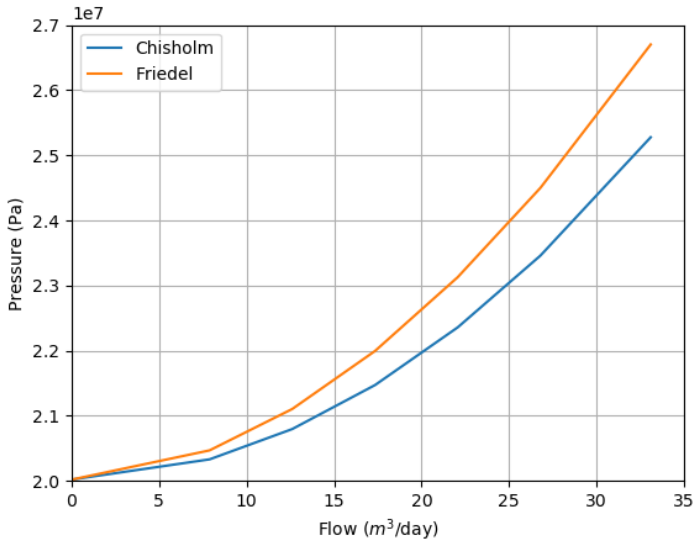

Source: author.

5. Conclusion and future works

5.1. Conclusion

The petroleum industry has to deal with a lot of challenges and uncertainties, especially during the production of fluids in the open sea. In this situation there are no sensors and equipment with which it is possible to measure the physical properties of the flux along the lift of the fluids to the platform. One can only know the flow rate, pressure and other parameters in the boundaries of the pipeline (at the platform and at the christmas tree), which are actually measured. Nevertheless, the flow of petroleum throughout the flowline and riser presents a multiphase behaviour and, because of that, there may be a lot of instabilities that can compromise the equipment and the whole production. The pressure versus temperature graphs are very important to the diagnosis of the behaviour inside the pipelines, especially when there is more than one phase flowing.

Thus, the algorithms presented in this work, used to integrate the pressure along all of the pipeline, have a great importance in predicting and preventing instabilities and severe slugging. They are less complex than the usual mechanistic algorithms presented in literature and used in commercial applications, and still, they have good reliability. Those algorithms are used to generate the graphs to understand the properties of the flow.

As the parameters to the integration are not directly observed, several correlations of flux and petroleum properties were considered and analysed in order to select the best ones. In the evaluation of the work it was used void fraction correlation of Bhagwat and Ghajar (2013), fluid properties from Standing (1947) and Ahmed (2001), well known by the industry, and two propositions of pressure drop by Chisholm (1973) and by Friedel (1979). The correlations and integration were done using field data from Andreolli (2018). He presents information to several situations and boundary conditions that were used to integrate the pressure.

The result of the plain integration showed a great performance, velocity and repeatability of the algorithm. The graphs presented prove that the curve format is well preserved and it can be applied to different cases. It was also compared the “direct” and “indirect” integration, starting from the separator and from the wet christmas tree, respectively, to demonstrate the robustness of the algorithm. There is an error in the algorithm

that occurs in all of the simulations, but the general shape and the shift between them is constant.

In order to understand the error, it was analysed the influence of the pressure drop correlations in the estimated pressure error and the correlation with the parameters of the field data. Then it is possible to know which pressure drop proposition presents the best adjustment and, apart from that, what is the main probable cause of error among the modelations of the parameters. The curves for Chisholm and for Friedel correlations showed that Chisholm proposes a more efficient and accurate pressure drop correlation and error is mainly due to the *WOR* model, which considers a constant behaviour of water along the oil production.

In addition to all of that, it was computed the pressure related to the initial *GOR* and the initial flow rate *Q* throughout the pipelines. They are important because it is possible to see the different curves for each value of *GOR* or *Q* and how they influence the pressure. In a general sense, the higher the *GOR* or the *Q* the higher is the pressure, as there are more fluids inside the tubes. With those initial data, it is possible to predict the probable pressure that the fluids can have inside the pipelines and use this information to make decisions. And finally, it was analysed the TPR curves of the system: in a specific point of the pipeline, in this case the wet christmas tree, the pressure is calculated to different values of initial flow rate. As expected, the pressure increases the higher the flow rate, but not in a linear way. Then, one can analyse the punctual behaviour of pressure in determined nodes of the pipeline and use that information to determine the best policies for the production.

5.2. Future works

The following suggestions are considered for future works:

i) include gas lift models along the pipelines;

ii) include a more accurate *WOR* modeling along the pipelines.

Bibliography

ABDALLAH, Muhammad Said. **PETE 402 Reservoir Simulation**. Saudi Arabia: King Fahd University of Petroleum & Minerals, 2017. DOI: https://doi.org/10.13140/RG.2.2.25642.00962.

ADDIS, M.A. Reservoir Depletion and Its Effect on Wellbore Stability Evaluation. **International Journal of Rock Mechanics and Mining Sciences**. 34th ed. April 1997.

AHMED, Tarek H. **Reservoir Engineering Handbook**. 2nd ed. Boston: Gulf Professional Pub, 2001.

ANDREOLLI, Ivanilto. **Estabilidade linear aplicada ao escoamento multifásico de petróleo**. São Paulo: Universidade de São Paulo, 2018. DOI: https://doi.org/10.11606/T.3.2018.tde-16072018-091052.

BALIÑO, J.L.; BURR, K.P.; NEMOTO, R.H. Modeling and Simulation of Severe Slugging in Air–Water Pipeline–Riser Systems. **International Journal of Multiphase Flow**, São Paulo, v. 36, n. 8, p. 643-660, August 2010. DOI: https://doi.org/10.1016/j.ijmultiphaseflow.2010.04.003.

BHAGWAT, Swanand M.; GHAJAR, Afshin J. Similarities and Differences in the Flow Patterns and Void Fraction in Vertical Upward and Downward Two Phase Flow. **Experimental Thermal and Fluid Science**, v. 39, p. 213-227, 2012. DOI: https://doi.org/10.1016/j.expthermflusci.2012.01.026.

BHAGWAT, Swanand M.; GHAJAR, Afshin J. A Flow Pattern Independent Drift Flux Model Based Void Fraction Correlation for a Wide Range of Gas-Liquid Two Phase Flow. **International Journal of Multiphase Flow**, v. 59, p. 186-205, August 2013. DOI: https://doi.org/10.1016/j.ijmultiphaseflow.2013.11.001.

BRENNEN, Christopher. **Fundamentals of Multiphase Flow**. April 2005. DOI: https://doi.org/10.1017/CBO9780511807169. ISBN: 9780511807169.

COLEBROOK, Cyril Frank. Turbulent Flow in Pipes, with particular reference to the Transition Region between the Smooth and Rough Pipe Laws. **Journal of the Institution of Civil Engineers**, v. 11, n. 4, p. 133-156, February 1939.

CHISHOLM, D. Pressure Gradients Due to Friction During the Flow of Evaporating Two-Phase Mixtures in Smooth Tubes and Channels. **International Journal of Heat and Mass Transfer**, Scotland, n. 2, p. 347-358, February 1973. DOI: https://doi.org/10.1016/0017-9310(73)90063-X. ISSN: 0017-9310.

EL-BANBI, Ahmed; ALZAHABI, Ahmed; EL-MARAGHI, Ahmed. **PVT Property Correlations: Selection and Estimation**, USA: Gulf Professional Pub, 2018.

FRIEDEL, L. Improved friction pressure drop correlations for horizontal and vertical two-phase pipe flow. **European two-phase flow group meeting**, Paper E2, Ispra 1979.

GANAT, Tarek Al-arbi; ULLAH, Najeeb; OTCHERE, Daniel Asante; ALI, Imtiaz. Develop Optimum Gas Lift Methods To Improve Gas Lift Efficiency Using Gas Lift Pack-Off, Deep Gas Lift, And Deep Lift Set. **International Journal of Advanced Research In Engineering & Technology**, n. 11, p. 1096-1114, December 2020.

GODA, Hiroshi; HIBIKI, Takashi; KIM, Seungjin; ISHII, Mamoru; UHLE, Jennifer. Drift-Flux Model for Downward Two-Phase Flow. **International Journal of Heat and Mass Transfer**, v. 46, n. 25, p. 4835-4844, May 2003. DOI: https://doi.org/10.1016/S0017-9310(03)00309-0.

ISHII, Mamoru; HIBIKI, Takashi. Drift-Flux Model. In **Thermo-Fluid Dynamics of Two-Phase Flow**, p. 345–79, Springer, 2006.

JONES, Owen C.; ZUBER, Novak. Statistical methods for measurement and analysis of two-phase flow. **Proceedings of the International Heat and Mass Transfer Conference**, p. 200-204, September 1974. DOI: 10.1615/IHTC5.480.

LIU, Wei; TAMAI, Hidesada; TAKASE, Kazuyuki. Pressure Drop and Void Fraction in Steam-Water Two-Phase Flow at High Pressure. **Journal of Heat Transfer**, v. 135, p. 319-1195, August 2013. DOI: https://doi.org/10.1115/1.4023678.

McCain, William. **Properties of Petroleum Fluids**, 3rd ed. Oklahoma: PennWell Corp., 2017.

POTTER, Merle C.; WIGGERT, David C. **Mecânica dos Fluidos**. 3º ed. Thomson Learning, 2003. Available in: <https://www.cengage.com.br/ls/mecanica-dos-fluidos/>. ISBN: 978-85-221-0309-6.

RAPP, Bastian E. Chapter 9 - Fluids. In **Microfluidics: Modelling, Mechanics and Mathematics**, p. 243–263. Oxford: Elsevier, 2017. DOI: https://doi.org/10.1016/B978-1-4557-3141-1.50009-5.

SATTER, Abdus; IQBAL, Ghulam M. **Reservoir Engineering**. Gulf Professional Publishing, 2016. DOI: https://doi.org/10.1016/C2013-0-13485-X. ISBN: 978-0-12-800219-3.

STANDING, M. B. A Pressure-Volume-Temperature Correlation for Mixtures of California Oils and Gases. New York: **American Petroleum Institute**, in: Drilling and Production Practice. January 1947.

STANDING, M. B. **Volumetric and phase behavior of oil field hydrocarbon systems**. Dallas: SPE, 1981.

STANDING, M. B.; KATZ, D. L. **Density of natural gases**. Trans. AIME, v. 146, p. 140–149, 1942.

TAHA, Abdullah; AMANI, Mahmood. Importance of Water Chemistry in Oil and Gas Operations — Properties and Composition. **International Journal of Organic Chemistry**, n. 9, p. 23-26, February 2019. DOI: https://doi.org/10.4236/ijoc.2019.91003. ISSN: 2161-4695.

TAITEL, Yehuda. Stability of Severe Slugging. **International Journal of Multiphase Flow**, v. 12, n. 2, p. 203–217, 1986.

WALLIS, G.B. **One-Dimensional Two-Phase Flow**. McGraw-Hill Book Co, 1969.

WOLDESEMAYAT, Melkamu A.; GHAJAR, Afshin J. Comparison of Void Fraction Correlations for Different Flow Patterns in Horizontal and Upward Inclined Pipes. **International Journal of Multiphase Flow**, v. 33, p. 347-370, 2007. DOI: doi:10.1016/j.ijmultiphaseflow.2006.09.004.

University of São Paulo

Petroleum Engineering – Polytechnic School

Number: 9835561 USP **Data: 01/2022**

Steady-state solutions for multiphase flow elevation of oil, gas and water

Roberta Lerin Lovisi

Advisor: Prof. Rafael Gioria dos Santos

Summary paper related to the discipline PMI3349 – Trabalho de Conclusão de Curso II.
This paper was prepared as a requirement to complete the Petroleum Engineering graduation at Polytechnic School of University of São Paulo.

Template 2021v01.

Resumo

No trabalho em questão, é apresentado um algoritmo que integra a pressão hidrostática em escoamentos multifásicos (óleo, gás e água) ao longo de dutos de produção de petróleo no oceano. A análise da pressão é imprescindível para otimizar a produção de petróleo e garantir o dimensionamento correto dos equipamentos, no entanto, os modelos usados para descrever escoamentos multifásicos em ambiente comercial costumam ser muito complexos. Por isso, o método proposto neste trabalho compreende um modelo mais simples, mas igualmente satisfatório, para prever a pressão do escoamento baseando-se em características fáceis de se mensurar.

A análise apresentada é conduzida com uma abordagem linear e não-transiente, na qual é usado o modelo de *black oil* para caracterização da fase líquida e a fração de vazio é definida pela proposta de *drift flux* de Bhagwat e Ghajar (2013). As correlações de propriedades dos fluidos de Standing (1947) e Ahmed (2001) além da abordagem de perda de carga de Chisholm (1973) são também implementadas no algoritmo. Os testes são realizados em um *riser* e *flowline* discretizados com cerca de 2000 metros de profundidade com uma geometria de *lazy wave* a partir dos dados de campo apresentados em Andreolli (2018). O código apresenta uma proposta aberta (*open source*) e é escrito em *Python*.

A integração da pressão apresenta erros da ordem de 20% para casos de baixo *WOR* quando comparados com os valores mensurados, o que é um erro aceitável. Além disso, análises das taxas de GOR e de vazão demonstram que óleos mais leves e com maiores fluxos têm uma perda de carga maior. Os resultados no geral contêm diversas análises do gradiente de pressão em relação a alguns parâmetros do fluxo e demonstram uma boa repetibilidade e robustez do algoritmo.

Abstract

In the present work, it is presented an algorithm to integrate the hydrostatic pressure of multiphase fluids (oil, gas and water) along a pipeline in the ocean during a petroleum production process. The pressure analysis is essential to optimize the production and guarantee the correct dimension of the equipment, but the commercial models used to describe multiphase flows are usually very complex. Therefore the method proposed in this work comprehends a simpler but just as satisfying model to predict the pressure of the flow based on easy-to-measure characteristics.

This analysis is conducted in a linear and non-transient approach, in which the black oil model is used for the characterization of the liquid phase and the void fraction is defined by the drift flux described by Bhagwat and Ghajar (2013). The correlations for fluid properties from Standing (1947) and Ahmed (2001) and pressure drop approach from Chisholm (1973) are applied in the algorithm. The tests are done in a discretized riser and flowline of around 2000 meters depth with a lazy wave geometry,

using field data from Andreolli (2018). The code presents an open source proposal and is written in Python.

As a result, the pressure integrated presents an error of around 20% in scenarios of low WOR, when compared to measured values, which is an acceptable value. Moreover, analyses of the GOR and flow rate show that lighter oils and higher rates present a higher pressure drop, and the algorithms can help predict those losses in order to dimensionate the flux. In general, the results contain several analyses of the gradient pressure related to some parameters of the flow and show a great repeatability and robustness of the algorithm.

1. Introduction

Petroleum is an important commodity and one of the most used energy sources in the world. The oil, however, is a mixture of hydrocarbons, water and other molecules formed over a thousand years in very specific environments and conditions. In Brazil, the petroleum is exploited mostly on the coast under a water depth of up to 3000 meters. Due to the different conditions of the environments, the oil that comes from the reservoir passes through various transformations before reaching the platform on the surface. The initial one-phase mixture turns to a multiphase flow while flowing through the production pipelines. In this way through the flowline and riser, the petroleum can be identified as a mixture of oil, water and gas.

Usually the water and oil are considered the same liquid phase and the gas can be in solution in the liquid phase or free in a second phase, which is called void fraction. Depending on the pressure and temperature to which this mixture is subjected inside the lines, there can be more or less phases. When the black oil is inside the reservoir it is basically only oil, when it is in a milder environment, with lower pressure and temperature, the gas that was in solution with oil is released and forms the void fraction, while the liquids tend to split in different phases because of the difference of density. The multiphase flow presents some challenges such as instability due to downward flow, also known as severe slugging. It can increase the pressure on the wellhead, trigger large instantaneous flows and flux oscillations in the reservoir, according to Andreolli (2018).

All those effects can cause serious damage on the equipments and disturb the petroleum production if not treated correctly. So, in order to achieve the maximum oil production, it is important to predict when and where are the points with the most probability of suffering severe slugging and to implement the appropriate methods to avoid and/or correct the issue. One of the ways to identify it is to model the petroleum flow through the pipelines and map the curves of pressure, in function of some parameters.

1.1. Void fraction

The void fraction (α), among all two-phase flow parameters (flow pattern, pressure drop, heat transfer, etc.), is one of the most important as it is used in almost all calculations of this type of flow. Nevertheless, the models that use void fraction are mostly developed to specific pattern flows (mainly horizontal and vertical orientations), or they need additional inputs related to the pattern flow. Because of that, Bhagwat and Ghajar (2013) suggest a drift flux model correlation for calculating the void fraction that is independent of the flow pattern and pipe orientation over a wide range of system pressures, pipe, diameters and fluid properties. The one dimensional drift flux to determine void fraction is presented in Equation (1), there j_A is the superficial velocity of the gas phase, C_0 is the distribution parameter, j_m is the mixture velocity and j_{AB} is the drift velocity.

$$\langle \alpha \rangle = \frac{\langle j_A \rangle}{C_0 \langle \langle j_m \rangle \rangle + \langle \langle j_{AB} \rangle \rangle} \tag{1}$$

1.2. Pressure drop

In an ideal system, the energy is always conserved and the velocity and the flow flux would not be affected by friction, shear and other non-conservative elements. However, in every real application of multiphase flow there is pressure drop. The two-phase component Φ_f^2 and the Fanning friction factor f_l in Equation (8), presented in Section 2, are the coefficients that comprehend the pressure drop. The correlations from Chisholm (1974) and Friedel (1979) present two approaches to the two-phase multiplier and are shown in Equation (2) and Equation (3) respectively. The Fanning friction factor is calculated by the Colebrook (1939) equation.

$$\phi_F^2 = A_1 + \frac{3.24 \times A_2 \times A_3}{Fr^{0.045} \times We^{0.035}} \tag{2}$$

$$\phi_F^2 = 1 + \left(\Gamma^2 - 1\right) \left\{ B \times x^{\frac{2-n}{2}} \times (1-x)^{\frac{2-n}{2}} + x^{2-n} \right\} \tag{3}$$

In those equations, *Fr* and *We* are the Froude and Weber numbers, that are relative respectively to the gravitational forces and to the surface tension of the fluids, Γ is the physical property coefficient, *x* is the mass quality, and A_1, A_2, A_3, *B* and *C* are auxiliar coefficients.

1.3. Properties of fluids

The petroleum fluids in a formation are very different from one another and depend on the type of sediments and process that made it become the oil found there. They are basically divided into reservoir models of gas and of oil. Among them there are other subtypes of fluids, which, according to McCain (2017), are: retrograde gas, wet gas, dry gas, volatile oil and black oil. The one used in this work is the ordinary black oil. They are present in nearly every basin and constitute the majority of the petroleum produced around the world. Because it is heavy and there are large molecules in its composition, it is found as 100% liquid (or undersaturated) inside the reservoir, where the pressure and temperature are high.

Some of the most important characteristics observed in the fluids are the formation volume factors. They represent how much of a determined fluid has to be exploited from the reservoir in order to produce 1 stock tank barrel at the surface condition. It is important because two events occur when they reach the surface – i) the release of free gas and ii) expansion of the fluid due to reduction of pressure and contraction due to reduction in temperature. Only i) is relevant to the changes in volume of oil, but not so important with water. In ii) the expansion and contraction of oil basically cancel each other and their effect is minimal (El-Banbi et al., 2018), but it is a relevant effect for the water (Taha and Amani, 2019). Those correlations, based on Ahmed (2001), are presented in Equation (4), Equation (5) and Equation (6).

$$B_o = \begin{cases} 0.9759 + 0.00012 \left[C_1 R_{so} \left(\frac{\gamma_g}{\gamma_o} \right)^{0.5} + 1.25 C_3 \right] & if\, P < P_b \\ B_{ob}^{-\frac{-1433 + 5\, C_1\, GOR + 17.2\, C_3 - 1180\, \gamma_g + 12.61\, API}{P \times 10^5} (P - P_b)} & else \end{cases} \tag{4}$$

$$B_w = A_1 + A_2 \times P + A_3 \times P^2 \tag{5}$$

$$B_g = \frac{P_0\, T\, z}{P\, T_0\, z_0} \tag{6}$$

The solution gas-oil ratio R_{so} is the quantity of gas produced to each barrel of oil. Once the reservoir is at or above the bubble pressure, the R_{so} remains constant and equal to the gas oil-ratio (*GOR*). The *GOR* is the gas-oil ratio at standard conditions for a petroleum produced in a reservoir at bubble pressure. The typical curve for that property is defined in Equation (7), proposed by Standing (1947).

$$R_{so} = \begin{cases} \frac{\gamma_g}{C_1} \left[\left(\frac{C_2\, P}{18.2} + 1.4 \right) \times 10^a \right]^{1.2048} & if\, P < P_b \\ GOR & else \end{cases} \tag{7}$$

2. Methodology

The methodology proposed for the accomplishment of the work consists of calculating the pressure in discrete nodes of the pipes that take the petroleum from the wellhead until the platform (riser and flowline) by numerical integration of the pressure drop. In order to do so, the terms of the Equation (8) are analysed separately and each of them is calculated, graphically evaluated and compared to literature values for validation. Some articles and papers were reviewed and their methods and equations selected so that proper correlations are applied to the model. As prior assumptions, it was considered that the liquids are incompressible, that the gas is ideal and the system is isothermic. As noted by Andreolli (2018), the discretization of the pipeline in more or less nodes does not have a big influence on the result of the integration. The physical and chemical correlations used are discussed in next sections: void fraction and drift flux from Bhagwat and Ghajar (2013), properties of fluids from Standing (1947) and Ahmed (2001) and for pressure drop it was considered the approaches from Friedel (1979) and from Chisholm (1973). Their results and graphical representation were calculated and computed using the data from Andreolli (2018) and Liu et al. (2013), and then compared with the results obtained in the books and papers consulted.

The hydrostatic pressure of the fluid inside the production pipe increases as it approaches the lower point at the seabed level. However, this increase in pressure is not linear and it depends on the vertical distance of the point considered to the surface and on the properties of the petroleum, such as the density. The gradient pressure defines the incremental amount of pressure to an infinitesimal distance. It is calculated according to the Equation (8) and integrated for small distances at various iterations. The properties of the fluid also depend on the pressure, so at each iteration, the parameters of the multiphase flow are calculated according to the new pressure and used again to integrate the

gradient. This process is executed until it reaches the christmas tree at the bottom, or the surface in the opposite direction: starting from the christmas tree and reaching the separator.

$$\frac{\partial P}{\partial S} = -\rho_m \cdot g \cdot \sin\theta - \phi_f^2 \cdot \frac{f_l}{2} \cdot \frac{G^2}{\rho_L \cdot D_h} \tag{8}$$

In Equation (8), ρ_m is the density of the mixture, which comprehends oil, gas and water, and its correlation is presented in (9), ρ_l is the density of the liquid phase, presented in (10) and g is the gravity acceleration. The void fraction α and the two-phase multiplier Φ_f^2 are calculated using the correlations presented in posterior sections. Some other data are measured in the field and are presented in the next section, Equations (11) and (12) show how to calculate the oil and water fraction in the pipes.

$$\rho_m = \rho_g \alpha + \rho_o \alpha_o + \rho_w \alpha_w \tag{9}$$

$$\rho_l = \frac{\rho_o \alpha_o + \rho_w \alpha_w}{1 - \alpha} \tag{10}$$

$$\alpha_o = \frac{j_o}{j_o + j_w}(1 - \alpha) \tag{11}$$

$$\alpha_w = \frac{j_w}{j_o + j_w}(1 - \alpha) \tag{12}$$

The densities of water and oil at flow condition are calculated according to Equation (13) and Equation (14) respectively. There ρ_{w0}, ρ_{o0} and ρ_{g0} are the densities of water, oil and gas at standard conditions respectively; ρ_{o0} and ρ_{g0} are calculated in Equation (15) and Equation (16). In Equation (15), γ_{o0} is the specific gravity of oil at standard conditions, in Equation (16) z is the compressibility factor of real gases and R is the specific gas constant for dry air.

$$\rho_w = \frac{\rho_{w0}}{B_w} \tag{13}$$

$$\rho_o = \frac{\rho_{o0} + \rho_{g0} Rs_o}{B_o} \tag{14}$$

$$\rho_{o0} = \gamma_{o0} \rho_{w0} \tag{15}$$

$$\rho_{g0} = \frac{P}{R T z} \tag{16}$$

Some other important parameters to the solution of the expressions are the superficial velocities of the fluids (j_w, j_o and j_g), which are presented in Equation (17), Equation (18) and Equation (19). They are measured in m/s and through them it is possible to define the drift flux of the mixture. There B_w, B_o and B_g are the water, oil and gas formation volume factors, *WOR* is the water-oil ratio, *GOR* is the

gas-oil ratio, j_{o0} is the superficial velocity of oil at standard conditions and R_{so} is the solution gas-oil ratio.

$$j_w = B_w \times WOR \times j_{o0} \tag{17}$$

$$j_o = B_o \times j_{o0} \tag{18}$$

$$j_g = B_g \times j_{o0} \times (GOR - R_{so}) \tag{19}$$

The input data used to integrate the pressure along the pipes were obtained from Andreolli (2018) and consists of the vertical (z) and horizontal (x) distance of 21 points to the wet christmas tree, and the boundary conditions of 11 different conditions, containing: superficial velocity at standard conditions (j_{o0}), pressure at the wet christmas tree (P_{WCT}) and at the separator (P_{sep}), the gas-oil ratio (GOR), the water-oil ratio (WOR) and the temperature at reservoir. Each of these conditions are used in a simulation.

3. Results

3.1. Pressure integration

In this Section, it is presented the result of the plain pressure integration for one case among the simulations. The algorithm started the calculations from the separator, using its boundary conditions, until reaching the wet christmas tree. Figure 1 presents the pressure profile of the fluids inside the pipelines versus its length from the platform to the christmas tree. Around the point 6700 m, it is possible to see that there is an oscillation of the pressure due to the lazy wave of the riser, and in the flowline the pressure is almost constant, as the height is basically the same. In the data from Simulation 1 of Table 2, and applying the Chisholm two-phase multiplier correlation, using the initial pressure of 4.16 MPa the final value achieved was 24.22 MPa against 20.10 MPa of the measured data. The difference is about -20.47%, which means the algorithm achieved a pressure almost 20% higher than the measured one.

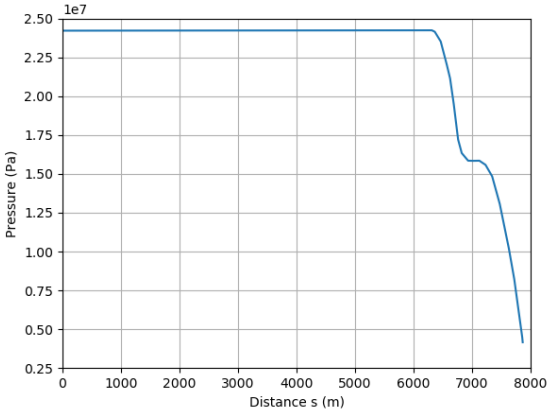

Figure 1 – Result of the forward integration of the pressure versus the length of the pipe. (Author)

3.2. Comparison of forward and backward integration

In order to test the algorithm, the same integration was executed backwards: starting from the wet christmas tree until reaching the platform, the result can be seen in the comparison of the integrations in Figure 2. The general format from the curves is preserved and they are shifted around 5 MPa from one another. This means that the integration method is robust and the equation is correctly employed. Then, it is possible to use this algorithm to calculate both the pressure at the platform and at the wet christmas tree, depending on the data available.

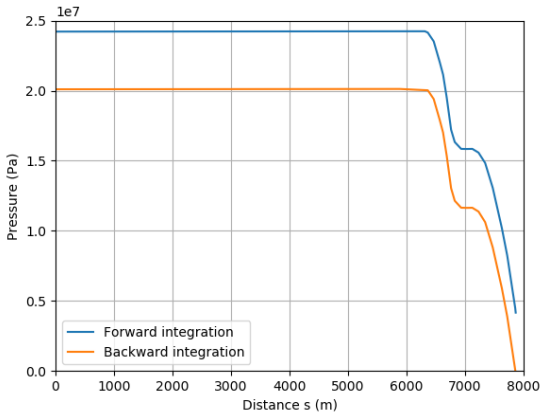

Figure 2 – Comparison of the results of the forward and backward integration of the pressure versus the length of the pipe. (Author)

3.3. Analysis of error

The errors of the estimated pressure in relation to the measured ones were computed and presented below with the purpose of analysing and understanding how it is behaving throughout the simulations.

Table 1 – Error of the estimated pressure for each simulation from Table 2.

Simulation	1	2	3	4	5	6	7	8	9	10	11
Error of the estimated pressure	-20,47%	-19,11%	-30,58%	-45,95%	-56,05%	-58,93%	-61,35%	-64,71%	-70,90%	-73,89%	-76,15%

The correlation between some of the parameters and the errors is presented in Table 2, and in Figure 3 it is possible to see the normalized value of the parameters (vertical left axis) in each simulation (horizontal axis) confronted with the errors (vertical right axis).

Table 2 – Correlation from some parameters with the error.

Parameter	j_{o0}	GOR	WOR	T
Correlation with error	96,87%	-13,16%	-97,24%	92,48%

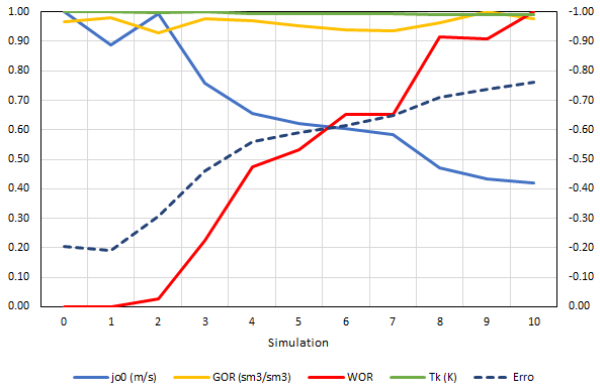

Figure 3 – Values of some parameters and of the error for each simulation. (Author)

It is possible to infer that the main cause of errors is the *WOR*. It is seen in both the graph from Figure 3 and in Table 2, in which the absolute correlation between error and *WOR* is the highest among the parameters, that as the water-oil ratio increases, the error increases in the negative axis. This assumption is reasonable once the model for water properties is not very robust and does not include variations of density and viscosity, for example. Along the riser, the change in pressure and temperature can also change the properties of water, but in this work those properties are considered constant.

3.4. Analysis of GOR quantity in the oil

In addition to the previous results, the pressure was plotted to different values of gas-oil ratio with the purpose of analysing the influence of *GOR* in the final result of the problem. The result is presented in Figure 4. To higher values, as the *GOR* increases, the distance between the curves also increases. As there is more gas dissolved in the oil, the mixture becomes lighter but more volatile, which also increases the general pressure inside the pipeline. Heavier fluids are less subject to height and temperature along the ocean's depth, which represents less tension in the pipe's inside walls.

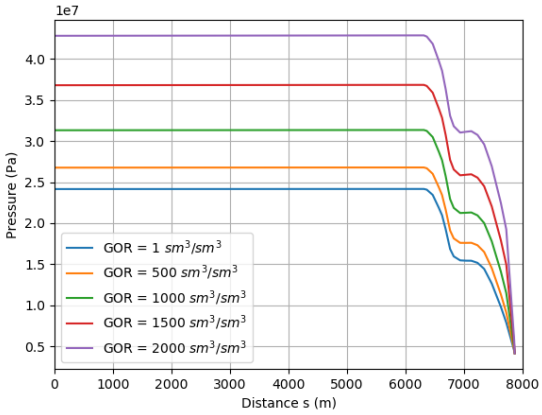

Figure 4 – Charts of the integration of the pressure versus the length of the pipe to different GOR values. (Author)

3.5. Analysis of the flow rate

An important way to evaluate the performance of the oil production is plotting the pressure against the flow rate of the fluids. The higher the flow rate, the higher is the amount of petroleum produced. However, the pressure inside the pipelines gets also higher as the flow rate increases and can cause problems during the production, as discussed above. Then, Figure 5 shows the curves of the

pressure as a function of the distance from the wet christmas tree. One can see that, as the flow rate increases, the pressure also increases, once there are more fluids flowing inside the same area.

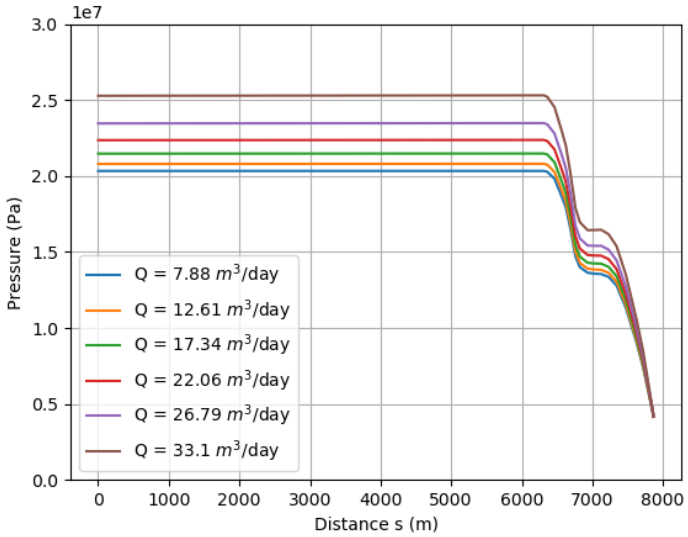

Figure 5 – Pressure plotted against distance from wet christmas tree to various values of flow rate. (Author)

Another important data that is considered in the analysis of the oil production are the Tubing Performance Relationship curves (TPR curves). They are used in nodal analyses and show the expected behaviour of the fluids in a specific node to various values of flow rate. The analysis at the wet christmas tree is presented in Figure 6, both two-phase multiplier correlations: from Chisholm and from Friedel.

It is possible to see that, as the flow rate decreases, the pressure also reaches a lower value, while it increases in a parabolic manner when the flow rate increases. The increase of the pressure is not so significant in the lower values of the flow rate because the friction within the tube is very high to lower fluxes and the pressure loss is equally high. However, as the inertia is overcome, the friction is not so relevant, thus the pressure has an ascendent behaviour.

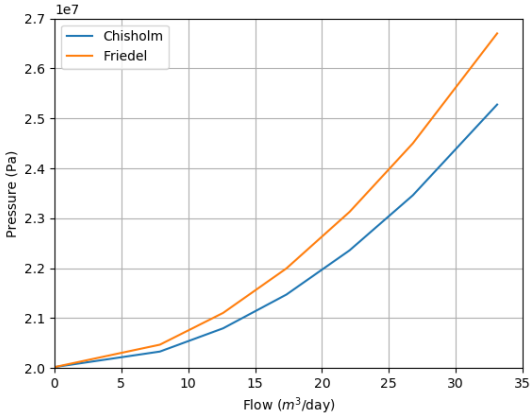

Figure 6 – TPR curves for Simulation 1 using Chisholm and Friedel two-phase multiplier. (Author)

4. Conclusion

Because of the lack of information throughout the whole production pipelines it is very difficult and complex to model and determine the fraction of fluids and their behaviour during the petroleum

production. One can only know with certainty the flow rate, pressure and other parameters in the boundaries of the pipeline (at the platform and at the christmas tree), which are actually measured. Nevertheless, those information are very important to the analysis of the pressure drop and other adversities inside the pipelines, especially when there is more than one phase flowing.

The algorithm presented in this work is less complex than the usual mechanistic algorithms found in literature and shows a great reliability in the results. The integrations showed a great performance, velocity and repeatability of the algorithm. The graphs presented prove that the curve format is well preserved and it can be applied to different cases of petroleum production. However the error is significant when considering high values of *WOR*, which indicates the high influence of water in the results and that the water modeling is not so accurate. The analyses of the pressure versus *GOR* and flow rate presented that lighter oils and higher rates present a higher pressure drop, and the algorithms can help predict those losses in order to dimensionate the flux. Those maps of pressure are important to predict the behaviour of fluids when the properties of the flow change and are very useful in the decision making process of a platform.

5. Bibliography

AHMED, Tarek H. **Reservoir Engineering Handbook**. 2nd ed. Boston: Gulf Professional Pub, 2001.

ANDREOLLI, Ivanilto. **Estabilidade linear aplicada ao escoamento multifásico de petróleo**. São Paulo: Universidade de São Paulo, 2018. DOI: https://doi.org/10.11606/T.3.2018.tde-16072018-091052.

BHAGWAT, Swanand M.; GHAJAR, Afshin J. A Flow Pattern Independent Drift Flux Model Based Void Fraction Correlation for a Wide Range of Gas-Liquid Two Phase Flow. **International Journal of Multiphase Flow**, v. 59, p. 186-205, August 2013. DOI: https://doi.org/10.1016/j.ijmultiphaseflow.2013.11.001.

COLEBROOK, Cyril Frank. Turbulent Flow in Pipes, with particular reference to the Transition Region between the Smooth and Rough Pipe Laws. **Journal of the Institution of Civil Engineers**, v. 11, n. 4, p. 133-156, February 1939.

CHISHOLM, D. Pressure Gradients Due to Friction During the Flow of Evaporating Two-Phase Mixtures in Smooth Tubes and Channels. **International Journal of Heat and Mass Transfer**, Scotland, n. 2, p. 347-358, February 1973. DOI: https://doi.org/10.1016/0017-9310(73)90063-X. ISSN: 0017-9310.

EL-BANBI, Ahmed; ALZAHABI, Ahmed; EL-MARAGHI, Ahmed. **PVT Property Correlations: Selection and Estimation**, USA: Gulf Professional Pub, 2018.

FRIEDEL, L. Improved friction pressure drop correlations for horizontal and vertical two-phase pipe flow. **European two-phase flow group meeting**, Paper E2, Ispra 1979.

ISHII, Mamoru; HIBIKI, Takashi. Drift-Flux Model. In **Thermo-Fluid Dynamics of Two-Phase Flow**, p. 345–79, Springer, 2006.

LIU, Wei; TAMAI, Hidesada; TAKASE, Kazuyuki. Pressure Drop and Void Fraction in Steam-Water Two-Phase Flow at High Pressure. **Journal of Heat Transfer**, v. 135, p. 319-1195, August 2013. DOI: https://doi.org/10.1115/1.4023678.

McCain, William. **Properties of Petroleum Fluids**, 3rd ed. Oklahoma: PennWell Corp., 2017.

STANDING, M. B. A Pressure-Volume-Temperature Correlation for Mixtures of California Oils and Gases. New York: **American Petroleum Institute**, in: Drilling and Production Practice. January 1947.

TAHA, Abdullah; AMANI, Mahmood. Importance of Water Chemistry in Oil and Gas Operations — Properties and Composition. **International Journal of Organic Chemistry**, n. 9, p. 23-26, February 2019. DOI: https://doi.org/10.4236/ijoc.2019.91003. ISSN: 2161-4695.